Molecular Biology of the Cell
Vol. 18, 3978–3992, October 2007

Exocyst Requirement for Endocytic Traffic Directed Toward the Apical and Basolateral Poles of Polarized MDCK Cells[D]

Asli Oztan,[*†] Mark Silvis,[†] Ora A. Weisz,[*†] Neil A. Bradbury,[‡] Shu-Chan Hsu,[§] James R. Goldenring,[‖] Charles Yeaman,[¶] and Gerard Apodaca[*†]

[*]Laboratory of Epithelial Cell Biology/Renal Electrolyte Division of the Department of Medicine and [†]Department of Cell Biology and Physiology, University of Pittsburgh, Pittsburgh, PA 15261; [‡]Department of Physiology and Biophysics, Chicago Medical School, Chicago, IL 60064; [§]Department of Cell Biology and Neuroscience, Rutgers University, Piscataway, NJ 08854; [‖]Department of Surgery and Cell and Developmental Biology, Vanderbilt University and the Nashville Veterans Affairs Medical Center, Nashville, TN 37212; and [¶]Department of Anatomy and Cell Biology, University of Iowa, Iowa City, IA 52242

Submitted February 2, 2007; Revised July 24, 2007; Accepted July 26, 2007
Monitoring Editor: Keith Mostov

The octameric exocyst complex is associated with the junctional complex and recycling endosomes and is proposed to selectively tether cargo vesicles directed toward the basolateral surface of polarized Madin-Darby canine kidney (MDCK) cells. We observed that the exocyst subunits Sec6, Sec8, and Exo70 were localized to early endosomes, transferrin-positive common recycling endosomes, and Rab11a-positive apical recycling endosomes of polarized MDCK cells. Consistent with its localization to multiple populations of endosomes, addition of function-blocking Sec8 antibodies to streptolysin-O–permeabilized cells revealed exocyst requirements for several endocytic pathways including basolateral recycling, apical recycling, and basolateral-to-apical transcytosis. The latter was selectively dependent on interactions between the small GTPase Rab11a and Sec15A and was inhibited by expression of the C-terminus of Sec15A or down-regulation of Sec15A expression using shRNA. These results indicate that the exocyst complex may be a multipurpose regulator of endocytic traffic directed toward both poles of polarized epithelial cells and that transcytotic traffic is likely to require Rab11a-dependent recruitment and modulation of exocyst function, likely through interactions with Sec15A.

INTRODUCTION

The generation and maintenance of epithelial polarity, which is indispensable for the functional integrity of epithelial tissues, requires sorting, transport, and delivery of newly synthesized and endocytosed proteins to the correct apical or basolateral plasma membrane domain (Yeaman *et al.*, 1999). The exocyst is an evolutionarily conserved eight-subunit protein complex (comprised of Sec3p, Sec5p, Sec6p, Sec8p, Sec10p, Sec15p, Exo70p, and Exo84p) that forms multiple protein–protein interactions and is required for tethering exocytic carriers to target membranes in eukaryotic cells (Munson and Novick, 2006; Wang and Hsu, 2006). In epithelial cells the exocyst is variably localized to the Golgi apparatus, the *trans*-Golgi network (TGN), recycling endosomes, and the junctional complex and is proposed to promote the targeting and fusion of biosynthetic and endocytic recycling cargo carriers with the basolateral plasma membrane domain, possibly at sites near the tight junction (Yeaman *et al.*, 2001, 2004; Folsch *et al.*, 2003; Prigent *et al.*, 2003).

Consistent with this model, addition of function-blocking antibodies to Sec8 inhibits delivery of newly synthesized proteins from the TGN to the basolateral, but not apical, surface of polarized Madin-Darby canine kidney (MDCK) cells (Grindstaff *et al.*, 1998). Overexpression of Sec10 stimulates the synthesis and delivery of basolateral, but not apical membrane proteins (Lipschutz *et al.*, 2000), whereas mutations in Sec5 or Sec6 inhibit trafficking of DE-cadherin from recycling endosomes to the basolateral domain of *Drosophila* epithelial cells (Langevin *et al.*, 2005). Furthermore, the RalA GTPase, which interacts with Exo84 and Sec5, is required for basolateral but not apical trafficking in polarized MDCK cells (Shipitsin and Feig, 2004), and AP1B, a basolateral-selective epithelial cargo adaptor, recruits the exocyst complex to recycling endosomes (Folsch *et al.*, 2003; Ang *et al.*, 2004). Although it has not been experimentally shown that basolateral recycling is exocyst dependent, interfering with Sec10 function or decreasing Sec5 expression interferes with recycling endosome morphology and transferrin (Tf) recycling in nonpolarized cells (Prigent *et al.*, 2003).

In contrast to the basolateral pathway, significantly less is understood about how targeted fusion is accomplished at the apical pole of epithelial cells, although numerous indi-

This article was published online ahead of print in *MBC in Press* (http://www.molbiolcell.org/cgi/doi/10.1091/mbc.E07–02–0097) on August 8, 2007.

[D] The online version of this article contains supplemental material at *MBC Online* (http://www.molbiolcell.org).

Address correspondence to: Gerard Apodaca (gla6@pitt.edu).

Abbreviations used: AEE, apical early endosome; ARE, apical recycling endosome; BEE, basolateral early endosome; CRE, common recycling endosomes; GFP, enhanced green fluorescent protein; MDCK, Madin-Darby canine kidney; pIgR, polymeric immunoglobulin receptor; PNS, postnuclear supernatant; SLO, streptolysin O; Tf, transferrin; TGN, *trans*-Golgi network.

rect data suggests that the exocyst may play some role in these events. The exocyst is localized to the primary cilium (Rogers *et al.*, 2004); it regulates Ca^{2+} signaling at the apical domain of pancreatic acinar cells (Shin *et al.*, 2000); it is required for targeting secretory vesicles to the rhabdomere (a densely packed tuft of microvilli located at the apical pole of the insect photoreceptor cells; Beronja *et al.*, 2005); it regulates exocytosis of apical secretory proteins in MDCK cells (Lipschutz *et al.*, 2000); it is associated with aquaporin-2 containing vesicles (which recycle at the apical pole of collecting duct principal cells; Barile *et al.*, 2005), and it may be involved in apical trafficking of Spdo/Notch/Delta (Jafar-Nejad *et al.*, 2005). Intriguingly, the exocyst may also modulate a form of "transcytosis," whereby DE-cadherin is delivered from the lateral membranes to the adherens junctions localized above the septate junction of insect epithelial cells (Langevin *et al.*, 2005). In mammalian epithelial cells, the adherens junction is localized below the tight junctions and transcytosis refers to the transfer of endocytosed membrane and solutes between the apical and basolateral poles of the cell; however, it is unknown whether the exocyst directs basolateral-to-apical transcytosis or other forms of apically directed endocytic traffic in these cells.

A potentially important link between endocytic traffic and the exocyst is the association between Sec15 and Rab11, a GTPase that regulates both biosynthetic and endocytic traffic (Wang *et al.*, 2000b; Ang *et al.*, 2003). Structural analysis has defined the site of *Drosophila* Rab11 interaction to a single helix in the C-terminal region of Sec15 (Wu *et al.*, 2005). The functional significance of the Sec15/Rab11 interaction is not well characterized, but overexpression of Sec15A-GFP in COS cells slows the egress of Tf from recycling endosomes (Zhang *et al.*, 2004), whereas in *Drosophila*, mutations in Sec5, Sec6, or Sec15 result in the accumulation of cargo in enlarged Rab11-positive endosomes (Beronja *et al.*, 2005; Langevin *et al.*, 2005). Rab11 is localized to the TGN and recycling endosomes of nonpolarized cells (Ullrich *et al.*, 1996; Ren *et al.*, 1998; Wilcke *et al.*, 2000). However, in polarized MDCK cells the majority of the Rab11 "a" isoform (Rab11a) appears to be localized to pericentriolar-localized apical recycling endosomes (ARE; Casanova *et al.*, 1999; Brown *et al.*, 2000; Leung *et al.*, 2000), where it regulates apical, but not basolateral, recycling and basolateral-to-apical transcytosis (Wang *et al.*, 2000b). Thus far, there is little information available regarding whether Sec15 and Rab11a interact in polarized mammalian epithelial cells or whether this interaction is of functional significance.

We observed that exocyst subunits were localized to multiple endocytic compartments and regulated basolateral-to-apical transcytosis, as well as apical and basolateral recycling pathways. Furthermore, our studies revealed that the C-terminus of Sec15A interacted with Rab11a and that expression of enhanced green fluorescent protein (GFP) fused to the C-terminus of Sec15A or down-regulation of Sec15A using short hairpin RNA (shRNA) impaired basolateral-to-apical transcytosis of IgA, but had no effect on receptor recycling pathways. Our results indicate that the exocyst is generally required for polarized endocytic traffic directed toward both poles of epithelial cells and that basolateral-to-apical transcytosis may depend on interactions between Rab11a and Sec15A.

MATERIALS AND METHODS

Antibodies

Ascites containing mouse mAbs against Sec8 (10C2, 5C3, or 2E12) were characterized previously (Grindstaff *et al.*, 1998), and used at 1:500 dilution for immunofluorescence (IF) labeling, 1:5000 dilution for Western blotting, and 1:100 dilution for streptolysin O (SLO) assays. The rSec6 and rSec8 mAbs (Stressgen, Ann Arbor, MI) were used at 1:100 dilution for IF labeling. Hybridoma supernatant containing the Sec15A mAb 15S2G6 was used undiluted for Western blotting. Hybridoma supernatant from cells expressing mouse monoclonal 13F3 antibody against Exo70 was used 1:10 dilution for IF labeling and Western blotting (Vega and Hsu, 2001). Hybridoma supernatant containing the Sec6 mAb 9H5 was used undiluted for Western blotting (Yeaman *et al.*, 2004). Ascites containing the anti-Myc 9E10 mAb (Dr. S. W. Whiteheart, University of Kentucky, Lexington, KY) was diluted 1:100 for use in SLO studies. Rat anti-ZO-1 hybridoma R40.76 culture supernatant (Dr. D. A. Goodenough, Harvard University, Cambridge, MA) was used at a dilution of 1:10. Serum containing anti-canine Tf antibodies (Apodaca *et al.*, 1994) was used at a 1:250 dilution for IF. Rabbit anti-EEA1 antibody (Dr. S. Corvera, University of Massachusetts Medical School, Worcester, MA) was used at a dilution of 1:500. An affinity-purified rabbit anti-Rab11 antibody specific for the N-terminus of Rab11 (ab3612; Abcam, Cambridge, MA) was used for immunoisolation. Mouse monoclonal anti-Rab11 antibody (610656; BD Transduction Laboratories, San Jose, CA) was used at 1:1000 dilution for Western blots. Anti-Rab11a-specific serum (Dr. J. Goldenring, Vanderbilt University, TN) was used for IF at a dilution of 1:500 for IF and 1:2500 for Western blotting. Rabbit anti-furin (Alexis Biochemicals, San Diego, CA) was used at a 1:500 dilution. Mouse monoclonal anti-Tf receptor antibody H68.4 (Invitrogen, Carlsbad, CA) was used 1:100 for IF and 1:2000 for Western blotting. Mouse anti-HA antibody (Covance, Berkeley, CA) was used in 1:250 for immunoprecipitation reactions. Mouse monoclonal anti-polymeric immunoglobulin receptor (pIgR) antibody Sc166 was used 1:100 for IF and 1:1000 for Western blots. Human polymeric IgA was purchased from Dr. J. P. Vaerman (Catholic University of Louvain, Belgium) and used at 0.2 mg/ml. All Cy5 and fluorescein isothiocyanate (FITC)-conjugated affinity-purified and minimal cross-reacting goat anti-mouse, -rabbit, -rat and -human secondary antibodies were purchased from Jackson ImmunoResearch Laboratories (West Grove, PA) and were used at 1:200 dilution. Cy3-conjugated secondary antibody (Jackson ImmunoResearch Laboratories) was used at 1:1000 dilution. For Western blotting, horseradish peroxidase (HRP)-conjugated goat anti-mouse and goat-anti rabbit secondary antibodies (Jackson ImmunoResearch Laboratories) were used at 1:10,000 and 1:50,000 dilutions, respectively.

DNA Constructs and Production of Adenoviruses

Full-length rat Sec15A, a 1170-base pair fragment (1–1170) encoding the first 390 amino acids of the N-terminus of Sec15A, or a 1296-base pair fragment (1171-2466) encoding the C-terminal 431 amino acids were cloned into the yeast two-hybrid vector pGADT7 (BD Biosciences, San Jose, CA) using BamHI and XhoI sites. For two-hybrid analysis Rab11a wild-type (Rab11a), dominant negative Rab11a-S25N (Rab11aSN), and dominant active Rab11a-S20V (Rab11aSV) were subcloned into the pBDGAL-Cam vector (Stratagene, La Jolla, CA) using standard DNA technologies. The GFP-Sec15CT chimera was generated by cloning the 1296-base pair fragment of Sec15A into the pEGFP-C3 vector (Clontech, Palo Alto, CA) using XhoI and BamHI sites. The GFP-Sec15CT(NA) construct was generated by mutating amino acid Asn_{709} to an alanine residue using the Quickchange Site-Directed Mutagenesis Kit (Stratagene). Adenovirus expressing GFP and triple hemagglutinin (HA)-tagged Rab11a (pAdTet-GFP/HA-Rab11a) was kindly provided by Robert Edinger (University of Pittsburgh). A recombinant adenovirus expressing GFP/HA-Rab11aSV was generated by mutating Ser_{20} in pAdTet-GFP/HA-Rab11a to a valine residue using the Quickchange Site-Directed Mutagenesis Kit (Stratagene) and the virus was produced as described previously (Henkel *et al.*, 1998).

Cell Culture, Generation of Stable Cell Lines, and Infection with Adenovirus

MDCK strain II cells expressing the wild-type rabbit pIgR (pWe) have been described (Breitfeld *et al.*, 1989). Cells were maintained in MEM (Cellgro, Herndon, VA) supplemented with 10% (vol/vol) fetal bovine serum (FBS; Hyclone, Logan, UT) and 1% penicillin/streptomycin in a 37°C incubator gassed with 5% CO_2. Cells were cultured on 12- or 75-mm, 0.4-μm Transwells (Costar, Cambridge, MA) as described (Breitfeld *et al.*, 1989a) and used 3–4 d after culture. Stable cell lines expressing GFP-Sec15CT or GFP-Sec15CT(NA) were created by transfecting MDCK-II cells with the appropriate vector using Lipofectamine 2000 reagent (Invitrogen, Carlsbad, CA) according to the manufacturer's instructions. Transfected cells were selected with 500 μg/ml G418. Cells were infected with recombinant adenovirus encoding the pIgR as described previously (Altschuler *et al.*, 2000). For GFP/HA-Rab11SV expression studies, cells were coinfected with one adenovirus that expressed GFP/HA-Rab11SV under the control of a tetracycline-regulated promoter and an additional adenovirus that expressed the tetracycline-repressible transactivator (AvTA) to induce expression in the absence of antibiotic (Henkel *et al.*, 1998).

IF Labeling, Confocal Microscopy, and Image Processing

When described, cells were permeabilized with 0.05% saponin in PIPES-KOH buffer (80 mM PIPES-KOH, pH 6.8, containing 2 mM $MgCl_2$, and 5 mM

EGTA) for 5 min at 4°C. Cells were fixed with methanol for 10 min at −20°C, with 4% (wt/vol) paraformaldehyde in 100 mM sodium cacodylate buffer (pH 7.4) for 10 min at room temperature or with a previously described pH-shift protocol (Bacallao and Stelzer, 1989; Apodaca *et al.*, 1994). After fixation with paraformaldehyde containing fixatives, unreacted paraformaldehyde was quenched with phosphate-buffered saline (PBS) containing 20 mM glycine, pH 8.0, and 75 mM NH_4Cl for 10 min at room temperature. Fixed cells were incubated with block buffer (0.025% [wt/vol] saponin, and 8.5 mg/ml fish skin gelatin in PBS) containing 10% (vol/vol) goat serum for 10 min at room temperature. Cells were incubated with primary antibody for 1 h at room temperature, washed three times with block buffer for 5 min, and then incubated with fluorescent-labeled secondary antibodies for 1 h at room temperature. After three additional 5-min washes with block buffer, the cells were rinsed with PBS, fixed with 4% paraformaldehyde in 100 mM sodium cacodylate, pH 7.4, for 5 min at room temperature and then mounted as described previously (Apodaca *et al.*, 1994). Imaging was performed using a TCS-SL confocal microscope (Leica, Deerfield, IL) equipped with argon, green helium-neon, and red helium-neon lasers. Images were acquired using a 100× 1.4 NA oil objective. Photomultipliers were set to 600–900 V and zoom at 4×. Images were collected every 0.25 μm and averaged three times. The images (512 × 512 pixels) were saved in a TIFF format and compiled using Volocity software (Improvision, Lexington, MA).

Immunoisolation of Rab11- and Sec8-positive Endosomes and Western Blotting

An "early" endosome fraction was enriched as described previously (Gorvel *et al.*, 1991). Preliminary results confirmed that this fraction was also enriched in Rab11-positive endosomes. Briefly, filter grown cells (cultured on 75-mm Transwells) were washed with ice-cold PBS, gently recovered by scraping into PBS, and recovered by centrifugation. The cells were resuspended in 300 μl of homogenization buffer (3 mM imidazole, pH 7.4, 250 mM sucrose, 0.5 mM EDTA, and complete proteinase inhibitor cocktail from Roche, Mannheim, Germany). Cells were homogenized by 21 strokes of a tight fitting Dounce homogenizer and then centrifuged for 10 min at 3000 rpm in a Heraeus Biofuge Fresco table-top centrifuge. The resulting postnuclear supernatant (PNS) was reserved, and the nuclear pellet was resuspended in an additional 300 μl of homogenization buffer and centrifuged again. The two PNS fractions were pooled, an aliquot was reserved for Western blot analysis, and the PNS was adjusted to 40.6% (wt/wt) sucrose using 62% (wt/wt) sucrose. The diluted PNS was placed in 12-ml capacity Polyclear centrifuge tubes and overlayed with 6 ml of 35% (wt/wt) sucrose and 4 ml of 25% (wt/wt) sucrose. The tubes were topped off with homogenization buffer and centrifuged in a TH-641 rotor at 108,000 × *g* for 3 h at 4°C. The endosome-enriched fraction (~1 ml) at the 25%/35% sucrose interface was collected with a needle.

Sheep anti-rabbit magnetic Dynabeads (50 μl; Invitrogen) were washed with 0.2% (wt/vol) bovine serum albumin (BSA) in PBS two times and incubated with 1 ml 5% (wt/vol) BSA in PBS overnight at 4°C. The following day the beads were recovered with a magnetic particle concentrator (Dynal, Oslo, Norway) and resuspended in 1 ml 5% BSA in PBS containing 5 μg of Rab11 polyclonal antibody (ab3612) or nonspecific rabbit IgG and incubated overnight at 4°C. The beads were washed with 1% (wt/vol) BSA in PBS, resuspended in ~2 ml of 5% BSA in PBS, and incubated with ~1 ml of the endosome fraction 3 h at 4°C on a rotator. The Rab11-positive endosomes associated with the Dynabeads were collected using a magnetic plate and washed two times with 0.2% BSA in PBS, and then one additional time with PBS. The endosome suspension was transferred to a new tube, magnetic beads were collected using a magnetic particle concentrator, and PBS was removed by aspiration. The endosomes bound to beads were boiled in Laemlli sample buffer and resolved on 15% SDS PAGE gel. Western blots were performed as described previously (Maples *et al.*, 1997). In some cases the blot was stripped using Restore Plus Western blot stripping buffer (Pierce, Rockford, IL) and then reprobed with different antibodies. For immunoisolation of Sec8-containing endosomal compartments, 5 μl of a 1:1:1 mixture of Sec8 antibodies (10C2, 5C3, and 2E12 ascites) was incubated with sheep anti-mouse magnetic Dynabeads. A nonspecific mouse IgG was used as a control. The immunoisolation was performed and samples were analyzed as described above.

Coimmunoprecipitation Analysis

Filter-grown MDCK cells were washed with ice-cold Ringer's saline (10 mM HEPES, pH 7.4, 154 mM NaCl, 7.2 mM KCl, 1.8 mM $CaCl_2$) twice, the filters were excised from their plastic holder and placed in Eppendorf tubes. A half milliliter of IP lysis buffer (50 mM Tris, pH 7.4, 150 mM NaCl, 5 mM EDTA, 10% glycerol, 1% NP-40, 1 mM PMSF, and 5 μg/ml pepstatin, leupeptin, and antipain) was added, and cells were lysed by vortex shaking for 10 min at 4°C. The supernatants were transferred into a new tube, a 1:500 dilution of anti-Sec8 antibody 10C2 was added and the samples were incubated overnight at 4°C on a rotator. Protein G Sepharose (Roche, Mannheim, Germany) was washed with ice-cold PBS, 50 μl of a 50% slurry was added to each tube, and the reaction was incubated at 4°C for 3 h on a rotator. Tubes were centrifuged 30 s at maximum speed in a 5414D microcentrifuge (Eppendorf, Westbury, NY), and the supernatants were aspirated. Beads were washed three times with IP lysis buffer and twice with low-salt wash buffer (2 mM EDTA, 10 mM Tris, pH 7.4) and then resuspended in 30 μl of 2× Laemmli sample buffer. The samples were heated at 95°C for 3 min and then centrifuged for 2 min to pellet the protein G beads. The cell lysate was resolved by SDS-PAGE and Western blots were probed with the indicated primary antibodies. For coimmunoprecipitation of Sec15CT with GFP/HA-Rab11SV, the cells were cross-linked with 0.2 μg/μl DSP (Pierce) at room temperature for 30 min before cell lysis. The reaction was stopped by incubating filters with 50 mM glycine at room temperature for 10 min, and then the cells were lysed and processed as described above. A 1:250 dilution of mouse anti-HA antibody and 50 μl of protein G Sepharose were added to the cell lysate and incubated overnight at 4°C on a rotator. Samples were centrifuged to pellet the beads and washed as described above. Before loading the samples on the gel, 10 μl of 1 M dithiothreitol (DTT) was loaded into each well to ensure reversal of the DSP cross-links.

SLO Permeabilization of MDCK Cells and Reconstitution of Membrane Trafficking in Semipermeabilized Cells

Basolateral recycling of ^{125}I-Tf in SLO-permeabilized cells was performed as described previously (Leung *et al.*, 1998). Delivery of IgA from the ARE to apical pole of the cell was performed as follows. ^{125}I-IgA was internalized from the basolateral surface of the cells for 10 min at 37°C, and the cells were then washed three times with MEM/BSA (minimal essential medium containing 20 mM HEPES, pH 7.4, 0.35 g/l $NaHCO_3$, 0.6% [wt/vol] BSA, and penicillin/streptomycin [1:100, Invitrogen-Invitrogen]) and then chased in ligand free medium for 20 min at 37°C. The cells were permeabilized with SLO (Murex Diagnostics, Norcross, GA) and transcytosis reconstituted as described previously (Apodaca *et al.*, 1996). To reconstitute apical recycling, cells were rinsed with warm MEM/BSA, and ^{125}I-IgA was internalized from the apical pole of the cell for 10 min at 37°C. The cells were washed three times with warm MEM/BSA and then two times with ice-cold MEM/BSA. The apical surface of the cells was treated with 25 μg/ml TPCK (tolylsulfonyl phenylalanyl chloromethyl ketone)-treated trypsin (in MEM/BSA) for 30 min at 4°C, rinsed with cold MEM/BSA, and then incubated with soybean trypsin inhibitor (125 μg/ml in MEM/BSA) for 20 min at 4°C. The cells were then permeabilized with SLO as described for the transcytosis assay. For each assay, control reactions were performed in the presence of cytosol, ATP, and an ATP-regenerating system. ATP independence was assessed by performing reactions in the presence of 40 U/ml apyrase (type VI; Sigma, St. Louis, MO) and cytosol, but lacking ATP and an ATP-regenerating system. For experimental samples, ascites containing function-blocking Sec8 mAbs (10C2, 5C3, and 2E12) or nonspecific Myc antibodies were included during the cytosol washout and during the reconstitution step (performed in the presence of cytosol, ATP, and an ATP-regenerating system). Experiments were performed 2–3 times in triplicate. ATP independent values were subtracted from control values and experimental values, and the resulting values were normalized to control reactions.

Yeast Two-Hybrid Screens

For yeast two-hybrid experiments the MATCHMAKER GAL4 Two-Hybrid System (Clontech) was used. Experiments were performed according to the directions supplied by the manufacturer.

Vesicle Budding

Reconstitution of vesicle-release from endosomes was performed as described previously (Bomsel and Mostov, 1993) with the following modifications. ^{125}I-IgA was internalized from basolateral surface of cells grown on 75-mm Transwell filters for 20 min at 18.5°C. The cells were washed with ice-cold MEM/BSA three times quickly and then three times 5 min on an orbital shaker at 4°C. The cells were then incubated at 37°C for 20 min to accumulate IgA in the ARE. After perforation with nitrocellulose, the cytosol was washed out in the presence of ascites containing anti-Sec8 mAbs (10C2, 5C3, 2E12) or anti-Myc mAb at 4°C for 45 min. Control reactions were reconstituted in the presence of an ATP-regenerating system and rat liver cytosol (2 mg/ml). ATP independence was assessed in reactions containing apyrase and cytosol. Experimental samples contained an ATP-regenerating system, cytosol, and either ascites containing the Sec8 or Myc mAbs. Data were analyzed as described above for the SLO assays.

Transfection of Polarized Filter-Grown Cells

Cells were plated on 12-mm Transwells, and 2 d later the medium was aspirated and replaced with low-calcium medium (DME-F12 medium containing 1.2 g/l $NaHCO_3$, 5 μM $CaCl_2$ and 10% [vol/vol] dialyzed FBS) and cultured for an additional 2 d. On the day of transfection, the low-calcium medium was aspirated, and the cells were incubated with PBS containing 1 mM $MgCl_2$ for 10 min at room temperature. Plasmid DNA (2–6 μg) and 4 μl of Lipofectamine 2000 (Invitrogen) were each diluted in 100 μl of Opti-MEM (Invitrogen-Invitrogen) and incubated for 5 min at room temperature. The DNA and Lipofectamine 2000 containing solutions were mixed and then incubated for 20 min at room temperature. Filters were placed on 40 μl drops of DNA/Lipofectamine complex (performed on Parafilm), and the remaining

160 μl of DNA/Lipofectamine complex was added to the apical well of the Transwell unit. Cells were incubated for 5–7 h at 37°C. An additional 900 μl of complete MEM medium containing 10% (vol/vol) FBS and penicillin/streptomycin/fungizone was added to the apical chamber, and 1.5 ml added to the well facing the basolateral surface of the cell. The cells were used 24-h after transfection.

IF Transcytosis Assay

Filter-grown cells were washed with MEM/BSA and incubated at 18°C for 15 min and pulsed with 200 μg/ml IgA from the basolateral surface of the cells for 20 min at 18°C. The cells were then placed on ice or incubated for 20 min at 37°C. During this chase, 25 μg/ml Cy3-labeled anti-human IgA was added to the apical media. The cells were then washed with ice-cold MEM/BSA and then PBS and finally fixed with 4% (wt/vol) paraformaldehyde in 100 mM sodium cacodylate, pH 7.4, for 10 min at room temperature. Cells were labeled as described above.

Postendocytic Fate of ^{125}I-Tf and ^{125}I-IgA

The postendocytic fate of a preinternalized cohort of ^{125}I-IgA or -Tf was performed as described previously (Breitfeld *et al.*, 1989; Maples *et al.*, 1997).

shRNA and RT-PCR Analysis in Polarized MDCK Cells

For shRNA studies, an algorithm from MIT (http://jura.wi.mit-.edu/bioc/siRNAext/home.php) was used to search for small interfering RNA (siRNA) sequences that were predicted to target splice-variants of canine Sec15A (XM_534966, XM_844233), but not Sec15B (XM_540235, XM_861541, XM_861551). Three candidate sequences were selected and custom-synthesized sense and anti-sense DNA oligos (IDT, Coralville, IA) were cloned into the pSuper.Neo.GFP vector (Oligoengine, Seattle, WA) according to the manufacturer's protocol. Cells were transfected with shRNA as described below and the efficiency of knockdown was assessed using Western blot, RT-PCR, and functional assays. One of the three constructs (pSuper-Sec15A) with target sequence AAGGAGAAATATATACCAAACTT was selected for further study. The other two sequences had little effect on Sec15A expression or in functional assays. The sequence of the 60-mer DNA oligos encoding the shRNA to the target sequence were as follows: sense strand (GATCCCCGGAGAAATATATACCAAACTTCAAGAGAGTTTGGTATATATTTCTCCTTTTTA) and anti-sense strand (AGCTTAAAAAGGAGAAATATATACCAAACTCTCTTGAAGTTTGGTATATATTTCTCCGGG). A negative control pSuper construct (pSuper-control) expressed a random construct with no known homology to canine sequences.

Early passage MDCK cells expressing the pIgR (pWe) were plated at low density to achieve 50–70% confluency at the time of transfection. The MDCK cells were trypsinized, resuspended in MEM culture medium, and recovered by centrifugation. Cells ($0.5–1.0 \times 10^6$) were resuspended in 100 μl of transfection buffer, which was prepared by mixing 20 μl of solution I (362 mM disodium salt of ATP, 590 mM $MgCl_2 \cdot 6H_2O$; stored at −80°C) with 1 ml of solution II (88.2 mM KH_2PO4, 14.3 mM $NaHCO_3$, 2.2 mM glucose, pH 7.4; stored at −20°C). The appropriate DNA construct (6 μg) was added to the cell suspension, and the cell/DNA mixture was placed into an Amaxa (Gaithersburg, MD) electroporation cuvette. Cells were nucleofected using the T-20 program. Immediately after transfection, 800 μl of MEM culture medium was added to the cells, the cells were resuspended using a sterile glass Pasteur pipette 6–8 times, and the cells were then plated in the apical chamber of collagen-coated 12-mm Transwell filters. MEM culture medium (1.5 ml) was added to the basolateral chamber, and the culture medium was aspirated and replaced 24 h after transfection. Experiments were performed 48 h after transfection.

For RT-PCR studies, mRNA was isolated from filter grown cells using an RNAqueous RNA isolation kit according to the manufacturer's protocol (Ambion, Austin, TX). cDNA was synthesized using 1 μg total RNA, oligo(dT) primer, and the M-MLV reverse transcriptase. For RT-PCR reactions, one fifth of the total cDNA reaction mixture was mixed with 5 mM dNTPs, 2 μM sense and anti-sense primers, and polymerase from the Expand High Fidelity PCR System (Roche). Canine Sec15A message was amplified using sense (GATGCTATTGGACAGTGAGT) and anti-sense (CTATGTATGCTGGGACATCCCAT) primers. To amplify canine Sec15B message, we used the following primers: sense (ACTTTTGCTGGAAGCTGAAG) and anti-sense (TCATGAGTGGTGGCTGCTGATGAGT). For RT-PCR the DNA was denatured at 94°C for 4 min followed by 25 cycles of amplification (94°C for 2 min, 55°C for 45 s, 72°C for 1 min) and finally 1 cycle of incubation for 5 min at 72°C. The complete PCR reaction was loaded on 1% agarose gel to observe amplified products. The gel pictures were scanned and quantified using QuantityOne software (Bio-Rad, Hercules, CA). For Western Blot analysis of shRNA-transfected cells, enhanced chemiluminescence reactions were exposed to film, and the images were quantified by densitometry using QuantityOne software. Background was subtracted from each well, values were normalized to actin or Sec8 expression, and the percentage decrease was calculated.

Statistical Analysis

Statistical significance was assessed using Student's *t* test. $p < 0.05$ was considered significant.

RESULTS

The Intracellular Pool of Exocyst Subunits Is Associated in Part with EEA1-, Tf-, and Rab11a-positive Endosomes But Not the TGN of Polarized MDCK Cells

Initial studies of exocyst subunit distribution in MDCK cells showed that Sec6 and Sec8 were localized at or near the tight junctions of cells after initiation of cell-to-cell contact or tubulogenesis (Grindstaff *et al.*, 1998; Lipschutz *et al.*, 2000; Rogers *et al.*, 2003). Other studies showed that the exocyst was associated with intracellular compartments including the Golgi, the TGN of MDCK cells expressing a kinase-inactive mutant of protein kinase D, and the recycling endosomes of wild-type MDCK cells (Yeaman *et al.*, 2001; Ang *et al.*, 2003; Prigent *et al.*, 2003). The discrepancy in exocyst localization may reflect, in part, the degree of cellular polarization, the growth conditions of the cells, the observation that some monoclonal antibodies differentially recognize pools of junctional versus intracellular populations of exocyst subunits (Yeaman *et al.*, 2001, 2004), and the possibility that the exocyst complex may exist in different conformational states (extended or closed) depending on its localization in the cell (Munson and Novick, 2006).

Using a number of fixation conditions and monoclonal antibodies to Sec6 (rSec6), Sec8 (rSec8, 10C2, 5C3, 2E12), and Exo70 (13F3), we found that permeabilizing cells with saponin (a treatment that removes the cytoplasmic pool of exocyst), just before fixation, revealed a large intracellular pool of exocyst subunits in polarized MDCK cells (see Supplementary Figures 1 and 2). This intracellular pool was also observed in preextracted, semipolarized MDCK cells grown on glass coverslips (data not shown). By removing soluble proteins, the extraction procedure may cause exocyst-interacting proteins to dissociate from the complex, thus allowing antibody binding. Alternatively, the extraction procedure may alter the conformation of the exocyst, revealing the intracellular pool of subunits. Importantly, the intracellular pool of Exo70 (and of Sec8 using the 10C2, 5C3, and 2E12 antibodies) was observed even in cells not permeabilized with saponin before fixation (see for example, Figures 1 and 3), confirming that the intracellular pool of exocyst is not simply an artifact of the saponin pretreatment.

We initially assessed whether there was colocalization between Sec8 (using mAb 10C2) or Exo70 (using mAb 13F3) and the TGN marker furin. The tight junction protein ZO-1 was labeled to mark the position of the apicolateral junction. Furin was localized to a ribbon-like structure that resided in a supranuclear position in the cell (Figure 1, A and C). We observed occasional regions where the furin-labeled TGN and Sec8 were in close proximity, but generally there was little colocalization between furin and Sec8 (Figure 1A). This lack of colocalization was also apparent for two other Sec8 antibodies (5C3 or 2E12) and Sec6 (data not shown). Exo70 was occasionally found associated with the ends of the TGN ribbons (see boxed region, Figure 1C), but there was generally not much overlap between Exo70 and furin (Figure 1C). Next, we analyzed if any of the exocyst-associated tubulovesicular elements were associated with EEA1-positive apical and basolateral early endosomes (AEE and BEE, respectively) (Leung *et al.*, 2000). Although there was no colocalization between EEA1 and Sec8 (Figure 1B), or EEA1 and Sec6 (data not shown), there appeared to be some localiza-

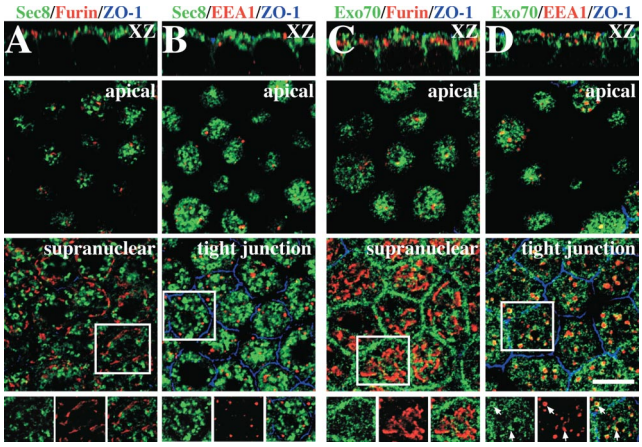

Figure 1. Localization of exocyst subunits in polarized MDCK cells. (A and B) Cells were treated with saponin and then fixed using a pH-shift protocol. (A) Distribution of Sec8 (green), furin (red), and ZO-1 (blue). (B) Distribution of Sec8 (green), EEA1 (red), and ZO-1 (blue). (C and D) Cells were fixed using the pH-shift protocol. (C) Distribution of Exo70 (green), furin (red), and ZO-1 (blue). (D) Distribution of Exo70 (green), EEA1 (red), and ZO-1 (blue). (A and D) An XZ section is shown in the top of each column, and single optical sections at the designated position of the cell are shown below. The bottom-most panels show the distribution pattern of exocyst subunits (green), and cellular markers (red) within the regions are marked with the white boxes. Scale bar, 10 μm.

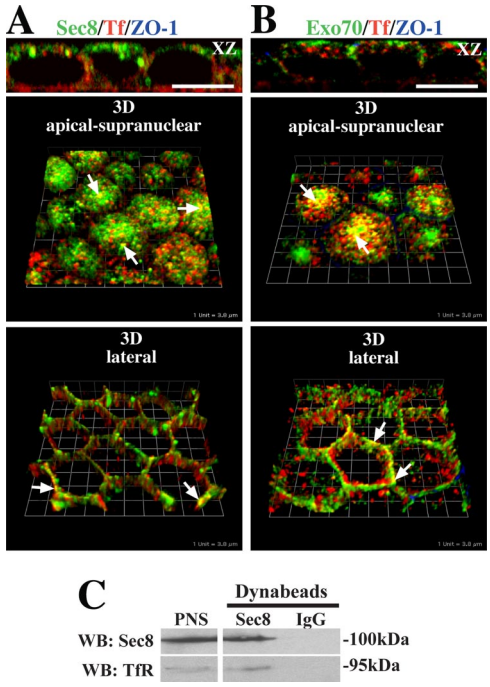

Figure 2. Association of exocyst subunits with Tf-positive endosomes. (A) Distribution of Sec8 (green), Tf (red), and ZO-1 (blue). (B) Distribution of Exo70 (green), Tf (red), and ZO-1 (blue). Top, an XZ section; middle, a 3D reconstruction of optical sections taken from the apical to supranuclear level of the cells; and bottom, a 3D reconstruction of optical sections taken along the lateral surfaces of the cells. Examples of colocalization between exocyst subunits and Tf-positive endosomes are marked by arrows. In XZ sections, the scale bar is equal to 10 μm. In 3-D reconstructions each length of the grid is equivalent to 3.8 μm. (C) Endosomal-enriched fractions were incubated with a pool of Sec8-specific antibodies (10C2, 5C3, 2E12) or IgG and recovered using Dynabeads coated with goat anti-mouse secondary antibodies. The lane at the left is a loading control showing that Sec8 and the Tf receptor were present in the starting PNS. The other lanes show the immunoisolated fraction bound to Sec8-specific antibodies or nonspecific rabbit IgG antibodies that were resolved by SDS-PAGE and then sequentially probed with antibodies to Sec8 or the Tf receptor. The immunoisolation protocol was performed three times, and results from one experiment are shown.

tion of Exo70 to EEA1-positive endosomes (Figure 1D). In this case, Exo70 appeared to concentrate at the periphery of the EEA1-positive endosomal elements (Figure 1D, inset).

We next examined whether Sec6, Sec8, or Exo70 were associated with Tf-positive BEE or the common recycling endosomes (CRE) of polarized MDCK cells. BEE are found closely apposed to the basal and lateral surfaces of the cell, whereas CRE are found in a peri- and supranuclear distribution (Sheff *et al.*, 1999; Wang *et al.*, 2000a). After basolateral uptake of Tf for 45 min, the cells were fixed and double-labeled with antibodies specific for canine Tf, Sec8, or Exo70. We observed some colocalization between the peripherally localized Tf-labeled BEE and the exocyst subunits (bottom panels, Figure 2, A and B). However, colocalization was more apparent for the Exo70 subunit. Colocalization was also readily observed in the supranuclear CRE (top panels, Figure 2, A and B), and Sec6 showed a similar degree of colocalization with Tf as that observed for Sec8 (data not shown). As further confirmation of our localization studies, we immunoisolated Sec8-positive endosome-enriched compartments and observed that the Tf receptor was associated with these membranes (Figure 2C). As a control we used nonspecific mouse IgGs, which failed to capture the Tf receptor.

The recent reports that Sec15 interacts with Rab11 (Zhang *et al.*, 2004; Wu *et al.*, 2005) prompted us to explore whether the exocyst was associated with the Rab11-positive ARE of polarized MDCK cells. The ARE, is morphologically distinct from the AEE, BEE, and CRE, is located at the apical pole of polarized MDCK cells, and is a site of regulation of apical recycling and basolateral-to-apical transcytosis of the pIgR (Apodaca *et al.*, 1994; Casanova *et al.*, 1999; Brown *et al.*, 2000; Wang *et al.*, 2000a). The pIgR normally transports basolaterally internalized IgA from BEE, to CRE, to the ARE, and then to the apical surface where the receptor is cleaved, releasing it along with bound IgA into secretions (Apodaca *et al.*, 1994; Brown *et al.*, 2000). However, a significant fraction of pIgR escapes proteolysis and is then endocytosed and recycled through the ARE en route to the apical cell surface. In our experiments, IgA was either internalized basolaterally for 10 min and chased for 20 min or internalized from the apical pole of the cell for 10 min, to accumulate ligand in the ARE. After apical uptake surface-bound ligand was removed by proteolysis, the cells were then fixed and labeled with antibodies specific for exocyst subunits, Rab11a, and IgA. We observed colocalization between Sec8 or Exo70 and Rab11a (Figure 3, A and C) or Sec8 or Exo70 with basolaterally internalized IgA (Figure 3, B and D). Triple label experiments confirmed that Sec8/Exo70, Rab11a and apically internalized IgA were codistributed in a subset of ARE (Figure 3, E and F).

Additional experiments confirmed the association of exocyst subunits with Rab11-positive endosomes and directly with dominant active Rab11aSV. An endosomal-enriched fraction was incubated with Dynabeads coated with an antibody that recognizes both a and b isoforms of Rab11 (the Rab11a specific antibodies we used for IF were not functional in this protocol). The immunoisolated fractions were resolved by SDS-PAGE and Western blots were probed with

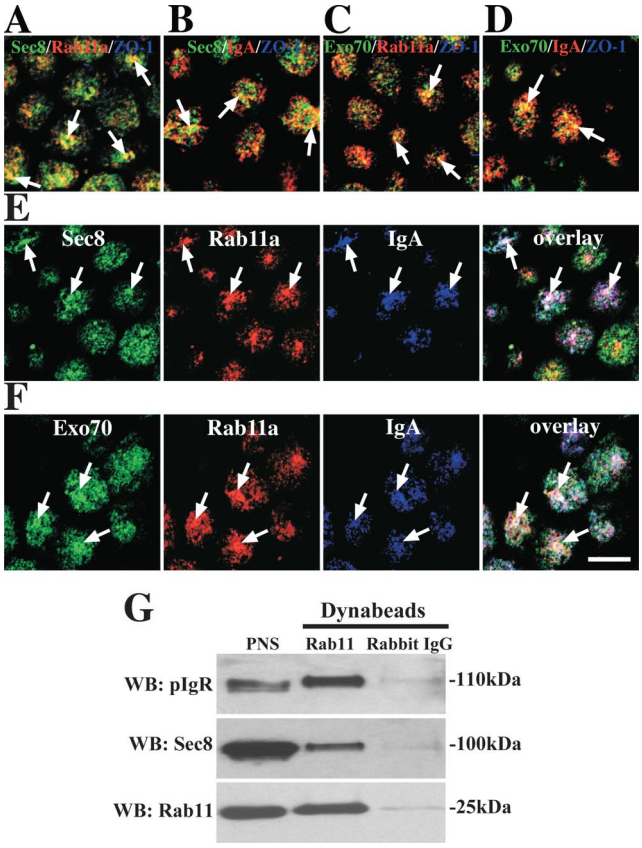

Figure 3. Localization of exocyst subunits to Rab11a- and IgA-positive recycling endosomes. (A–D) Distribution of Sec8/Exo70 (green) and Rab11a (A and C) or IgA (B and D). The distribution of ZO-1 was also examined but is not apparent in all of the panels. (B and D) IgA was internalized from the basolateral pole of the cell for 10 min and chased 20 min at 37°C. (E and F) IgA was internalized from apical pole of the cell for 10 min. (E) The cells were fixed and stained with antibodies to Sec8 (green), Rab11a (red), and IgA (blue). (F) Cells were stained with antibodies to Exo70 (green), Rab11a (red), and IgA (blue). In B and E cells were treated with saponin before fixation, whereas in A, C, D, and F cells were fixed before permeabilization. Arrows indicate areas of colocalization between the three markers. Scale bar, 10 μm. (G) Association of Sec8 and pIgR with immunoisolated Rab11-positive endosomes. The lane at the left shows that Sec8, pIgR, and Rab11 were present in the starting PNS, and the other lanes show the immunoisolated fraction bound to Rab11-specific antibodies or nonspecific rabbit IgG antibodies that were resolved by SDS-PAGE and then sequentially probed with antibodies to Sec8, pIgR, or Rab11. The immunoisolation protocol was repeated three times, and results from one experiment are shown.

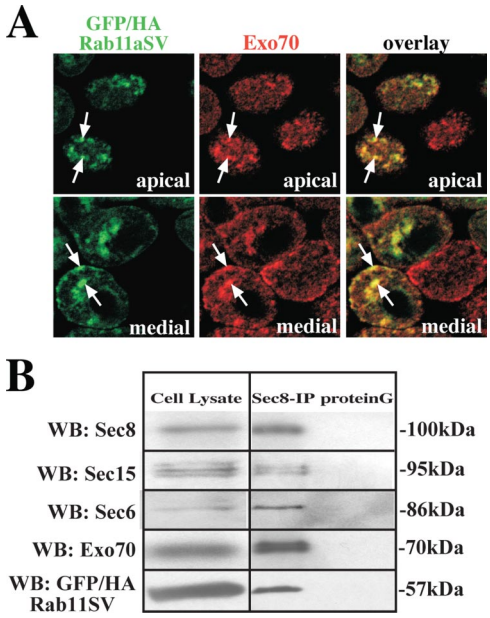

Figure 4. Association of exocyst subunits with GFP/HA-Rab11aSV. (A) MDCK cells were infected with virus encoding GFP/HA-Rab11aSV and then fixed and processed for IF. The distribution of GFP/HA-Rab11aSV (green) and Exo70 (red) are shown. A merged image is shown at the right. Scale bar, 10 μm. (B) Cells were infected with virus encoding GFP/HA-Rab11aSV, lysed, and Sec8 and associated proteins were immunoprecipitated using Sec8-specific mAb 10C2 or protein G alone. The cell lysate (one-twentieth of the total) or the immunoprecipitated proteins were resolved by SDS-PAGE, and a Western blot was sequentially probed with antibodies to Sec6, Sec8, Sec15, Exo70, and Rab11a. The coimmunoprecipitation protocol was performed two times and results from one experiment are shown.

pIgR-, Rab11-, and Sec8-specific antibodies (Figure 3G). Consistent with the IF analysis, a fraction of Sec8 and the pIgR was associated with Rab11-positive endosomes. Little pIgR, Rab11, or Sec8 association was observed in control reactions incubated with nonspecific rabbit IgGs (Figure 3G). The Golgi marker GM130 was not observed in the Rab11a-positive endosome fraction (data not shown), confirming that the immunoisolated sample represents an endosome-enriched fraction and does not pulldown other non–Rab11a-associated membrane-bound compartments.

Likely reflecting the transient nature of the Rab11a/exocyst interaction, we were unable to coimmunoprecipitate endogenous Rab11a with antibodies to Sec8, Sec15A, or Exo70. However, when we infected MDCK cells with an adenovirus encoding a GTPase-deficient mutant of Rab11a fused to GFP and containing an HA tag (GFP/HA-Rab11aSV), we observed that Exo70 was associated with GFP-Rab11aSV–positive endosomes (Figure 4A). Furthermore, when we performed coimmunoprecipitation using Sec8 antibodies, we observed that multiple exocyst subunits (Sec6/Sec8/Sec15A/Exo70) as well as GFP/HA-Rab11aSV were found in a complex (Figure 4B). Exo70 did not colocalize with a dominant negative mutant of Rab11a (GFP/HA-Rab11aSN), which appeared to be primarily cytosolic (data not shown).

Taken together, the above data indicate that exocyst subunits are localized to multiple endocytic compartments including early endosomes, Tf-positive recycling endosomes, and the Rab11a-positive ARE, but not to a significant degree with the TGN of polarized MDCK cells.

Basolateral Recycling, Apical Recycling, and Basolateral-to-Apical Transcytosis are Exocyst-dependent Trafficking Pathways

Next, we examined whether there was a functional role for the exocyst in postendocytic trafficking pathways. For this analysis we used SLO-permeabilized cell assays that we previously developed to measure transcytosis and recycling (Apodaca *et al.*, 1996; Leung *et al.*, 1998). Important advantages of this technique include the ability to examine exocyst function after the cells have already polarized, the ability to test the acute effects of inhibiting exocyst function on defined trafficking events and the ability to uniformly perme-

abilize the entire monolayer, ensuring equal delivery of the reagents to each cell.

We first examined whether Tf recycling in polarized MDCK cells was dependent on the exocyst. ^{125}I-Tf was internalized from the basolateral surface of filter-grown MDCK cells, the cells were permeabilized with SLO, and after cytosol washout, vesicle trafficking was reconstituted at 37°C in the presence of exogenous cytosol and an ATP-regenerating system. A pool of function-blocking Sec8 mAbs (10C2, 5C3, 2E12; Grindstaff *et al.*, 1998) was included in the washout step, and the reconstitution reaction. As a control we substituted the Myc 9E10 mAb for the Sec8 antibodies in the reaction. At the end of the reconstitution reaction, the percentage of ligand that was recycled was calculated. The

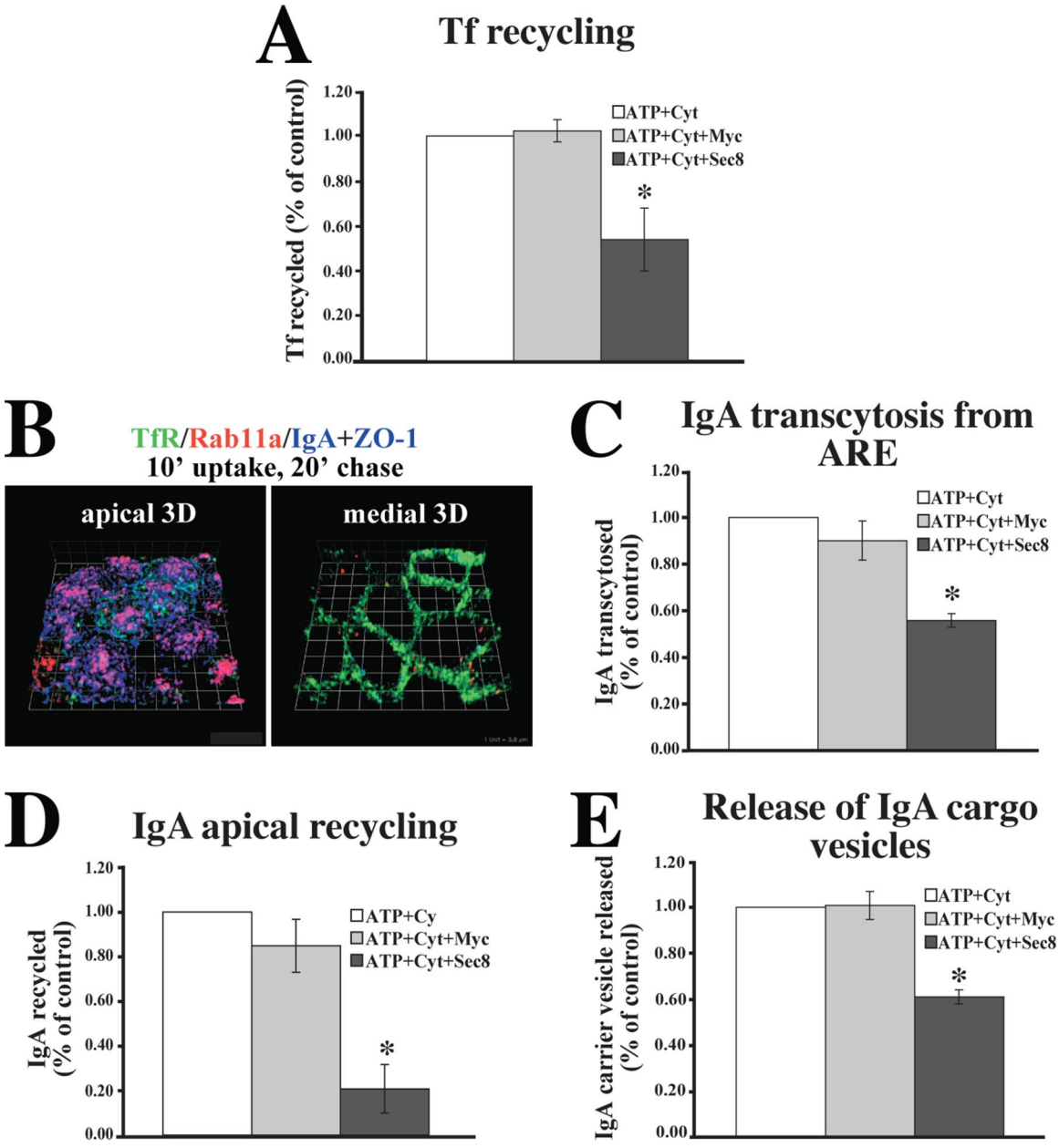

Figure 5. Exocyst requirement for endocytic traffic in SLO-permeabilized MDCK cells. (A) Basolateral recycling of ^{125}I-Tf in SLO-permeabilized MDCK cells incubated in the presence of an ATP-regenerating system (ATP), cytosol, and either Myc antibodies (Myc) or a pool of Sec8 antibodies (10C2, 5C3, 2E12). The ATP-independent fraction was ~12% and values for control reactions performed in the presence of an ATP-regenerating system and cytosol were ~46%. Data are mean ± SEM (n = 3; performed in triplicate). (B) IgA was internalized basolaterally for 10 min at 37°C, and the cells were incubated in the absence of IgA for 20 min. The cells were fixed and stained with antibodies to IgA (blue), ZO-1 (blue), Tf receptor (green), and Rab11a (red). 3-D reconstructions are shown. Each length of the grid = 3.8 μm. (C) Ligand was internalized as described in B, and apical release of ^{125}I-IgA was quantified in SLO-permeabilized cells. The ATP independent fraction was ~8%, and values for control reactions were ~42%. Data are mean ± SEM (n = 2; performed in triplicate). (D) Apical ^{125}I-IgA recycling in SLO-permeabilized cells. The ATP independent fraction was ~30%, and values for control reactions were ~47%. Data are mean ± SEM (n = 2; performed in triplicate). (E) Release of ^{125}I-IgA-labeled cargo vesicles from mechanically perforated MDCK cells. The ATP-independent fraction was ~8%, and values for control reactions were ~30%. Data are mean ± SEM (n = 3; performed in duplicate). *Statistically significant difference between reactions performed in the presence of Myc or Sec8 antibodies ($p < 0.05$).

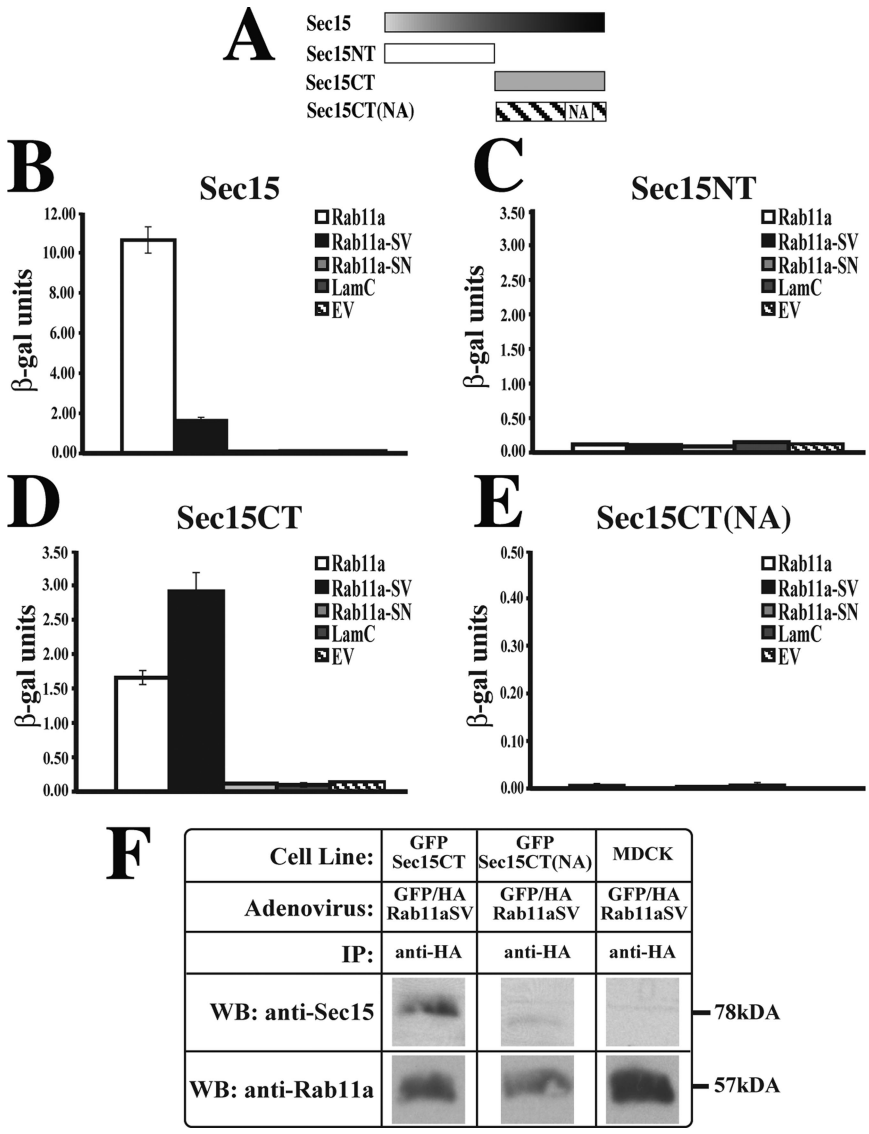

Figure 6. Interaction between Rab11a and the C-terminus of Sec15A. (A) Sec15A constructs used to identify the Sec15A-Rab11a interaction domain. (B–E) Results of CPRG assay between the Sec15A constructs shown in panel A and either wild-type Rab11a (Rab11a), dominant active Rab11a-SV, dominant negative Rab11a-SN, lamin C (LamC), or empty vector (EV). These assays were repeated two times. Data from one determination are shown. Mean ± SD (n = 3). (F) Untransfected MDCK cells or stable MDCK cells lines expressing GFP-Sec15CT or GFP-Sec15CT(NA) were infected with adenovirus encoding GFP/HA-Rab11aSV. The cells were cross-linked and lysed, and GFP/HA-Rab11aSV was immunoprecipitated with anti-HA antibodies. The immunoprecipitates were resolved by SDS-PAGE and Western blots were sequentially probed with antibodies that recognize Rab11a or Sec15A.

ATP-dependent values were normalized to control reactions that contained an ATP-regenerating system and cytosol, but no antibody. The addition of Sec8 antibodies significantly inhibited basolateral recycling of Tf by ~45%; however, no effect was observed upon addition of the nonspecific Myc antibody (Figure 5A).

In the next experiment, we examined whether transit of ^{125}I-IgA from the ARE and release from the apical pole of the cell was exocyst-dependent. ^{125}I-IgA was internalized for 10 min at 37°C, washed, and then chased for 20 min to accumulate IgA in the Rab11a-positive elements of the ARE. IF confirmed that under these internalization conditions, IgA was present at the apical pole of the cell in tubulovesicular structures that colocalized with Rab11a, but not with Tf receptor (Figure 5B). The cells were then permeabilized with SLO and ^{125}I-IgA release from the ARE was measured in the presence or absence of exocyst antibodies. Blocking antibodies significantly inhibited IgA trafficking from the ARE by ~40% (Figure 5C), whereas Myc antibodies had no effect.

As further confirmation that the exocyst modulated apically directed traffic, we also explored apical recycling of IgA in SLO-permeabilized cells. Filter-grown cells were pulsed with ^{125}I-IgA from the apical domain for 10 min, the cells were washed and chased in the absence of ligand for a total of 5 min, and then membrane bound IgA was stripped from the surface with trypsin at 4°C. The cells were permeabilized with SLO, and apical IgA release was reconstituted in the presence of Sec8 or Myc antibodies as described above. In the presence of the Sec8 antibodies, the pool of IgA that recycled apically and was dependent upon ATP and cytosol was significantly inhibited by ~80% relative to control (Figure 5D). It is worth noting that we observed a relatively large ATP independent pool of recycling IgA in these assays (~30%), indicating that either reconstitution was inefficient or that apical recycling had little requirement for ATP. The ATP-independent pool of recycling was insensitive to the addition of Sec8 antibodies (data not shown).

It was previously shown that apical delivery of newly synthesized p75 neurotrophin receptor was independent of exocyst function (Grindstaff *et al.*, 1998). Consistent with this previous analysis, we found that addition of function blocking Sec8 antibodies to SLO permeabilized MDCK cells had no significant effect on apical delivery of this protein (data not shown). This latter observation confirms that only a

subset of trafficking events are exocyst dependent in SLO-permeabilized cells.

Although the exocyst is generally thought to be involved in promoting transit between intracellular compartments and the plasma membrane, some studies indicate that it may also play a role in modulating cargo exit from the TGN or endosomes (Yeaman *et al.*, 2001; Beronja *et al.*, 2005; Langevin *et al.*, 2005). To explore this possibility, we reconstituted vesicle budding from ARE in mechanically perforated cells. ^{125}I-IgA was internalized basolaterally for 20 min at 18°C and then chased for 20 min to accumulate IgA in the ARE. The apical membrane was then mechanically perforated with nitrocellulose (Bomsel and Mostov, 1993) and release of ^{125}I-IgA in transport vesicles was measured in the presence of Sec8 or Myc antibodies, cytosol, and an ATP-regenerating system. Addition of antibodies against Sec8, but not Myc, resulted in a significant inhibition of ^{125}I-IgA release from labeled ARE (Figure 5E).

Taken together the above results indicate that the exocyst modulates a broad spectrum of endocytic trafficking events in polarized cells, including those directed toward the apical and basolateral pole of the cell. Furthermore, the exocyst may modulate the exit of IgA-pIgR cargo from the ARE.

The C-terminus of Sec15A Binds to Rab11a

The potential requirement for the exocyst in basolateral-to-apical transcytosis and apical recycling prompted us to further explore the molecular requirements for this dependence. We initially focused on the previously described interaction between Sec15 and Rab11 (Zhang *et al.*, 2004; Wu *et al.*, 2005). Although mapping of Sec15-Rab11 interactions was recently described using *Drosophila* proteins (Wu *et al.*, 2005), we confirmed these interactions with their mammalian orthologues (Figure 6). Using a two-hybrid approach and a quantitative β-galactosidase assay, we observed that full-length rat Sec15A interacted with wild-type Rab11a as well as with GTPase-deficient Rab11a-SV. However, no interaction was observed with the dominant negative mutant Rab11aS25N (Rab11a-SN), Lamin C, or empty vector (Figure 6B). Next, we broadly examined the region of Sec15A that was involved in these interactions. The Sec15A N-terminus (Sec15NT; amino acids 1–390) showed no interactions with Rab11a (Figure 6C). However, the Sec15A C-terminus (Sec15CT; amino acids 391–822) interacted, like the intact protein, with wild-type Rab11a and Rab11a-SV, but not with Rab11a-SN (Figure 6D). It was previously reported that a point mutation that converted Asn_{659} to an alanine residue in *Drosophila* Sec15CT blocked its interaction with Rab11 (Wu *et al.*, 2005). We observed that the analogous mutation in mammalian Sec15CT, in which Asn_{709} was converted to an alanine residue (Sec15CT(NA)), prevented the interaction of Rab11a with the C-terminus of Sec15A (Figure 6E).

To confirm that Sec15CT can interact with Rab11a in vivo, we generated stable cell lines expressing GFP-Sec15CT or GFP-Sec15CT(NA), which were subsequently infected with GFP/HA-Rab11aSV adenovirus. The cells were cross-linked with the reversible cross-linker DSP, lysed, and GFP/HA-Rab11aSV was immunoprecipitated using an anti-HA antibody. Western blots of the immunoprecipitates were probed with the 15S2G6 antibody (which recognizes the C-terminus of Sec15A) or with antibodies against Rab11a. Consistent with our two-hybrid analysis, anti-HA antibodies coimmunoprecipitated a complex between GFP/HA-Rab11aSV and GFP-Sec15CT, but little interaction was observed between GFP/HA-Rab11aSV and GFP-Sec15(NA) (Figure 6F).

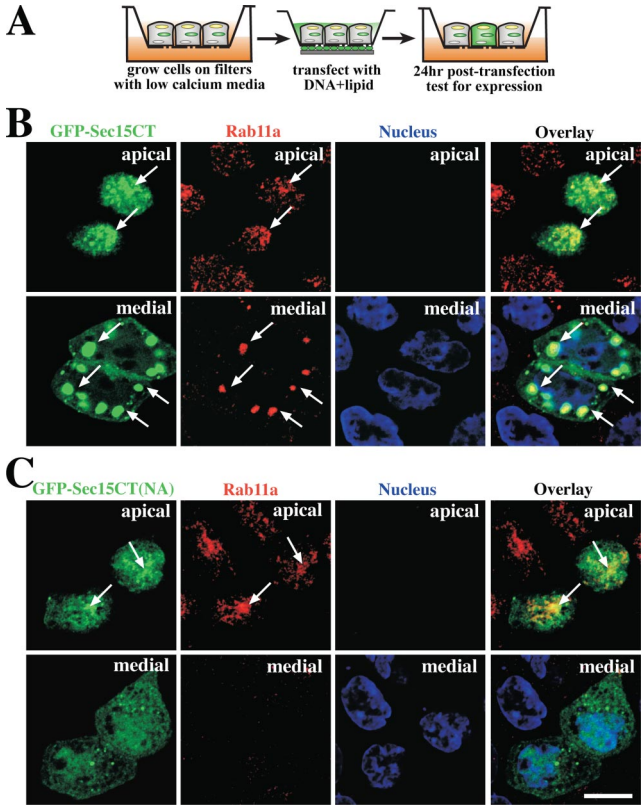

Figure 7. Expression of GFP-Sec15CT and GFP-Sec15CT(NA) in polarized MDCK cells. (A) Filter transfection protocol. (B) Distribution of GFP-Sec15 (green), Rab11a (red), and the nucleus (blue). (C) Distribution of GFP-Sec15(NA) (green), Rab11a (red), and the nucleus (blue). Individual optical sections from the apical or medial regions of the cell are shown. A merged image (overlay) is shown in the right-hand panels. Examples of colocalization between exocyst subunits and Rab11a are marked by arrows.

Expression of Sec15CT or Down-Regulation of Sec15A Impairs Basolateral-to-Apical Transcytosis of pIgR-IgA Complexes

We next examined whether Sec15CT expression affected the distribution of Rab11a, potentially by impairing interactions between endogenous Sec15 and Rab11a. We transiently transfected polarized filter-grown MDCK cells with GFP-tagged Sec15CT (GFP-Sec15CT), and ~24 h after transfection the cells were fixed and labeled with Rab11a-specific antibodies (Figure 7A). We estimate that ~20–30% of the cells expressed GFP-Sec15CT after transfection. We observed that GFP-Sec15CT was localized to small vesicular structures at the apical pole of the cell as well as very large "vesicular" structures in the medial cytoplasm. Rab11a colocalized with both pools of GFP-Sec15CT (Figure 7B), as did the pIgR (see Figure 8B). However, the large medial GFP-Sec15CT–positive elements did not colocalize with or alter the distribution of Sec8 nor did they colocalize with basolaterally internalized IgA (data not shown). When examined by live-cell imaging, GFP-positive vesicular elements were observed to enter and exit the large vesicular structures (data not shown), demonstrating that these structures are dynamic and unlikely to be cytoplasmic accumulations of GFP-Sec15CT in aggresomes. The mutant version of GFP-tagged Sec15CT (GFP-Sec15CT(NA)) showed some puncta at the apical pole of the cells that were positive for Rab11a (Figure 7C), indicating that the mutant may have bound to this

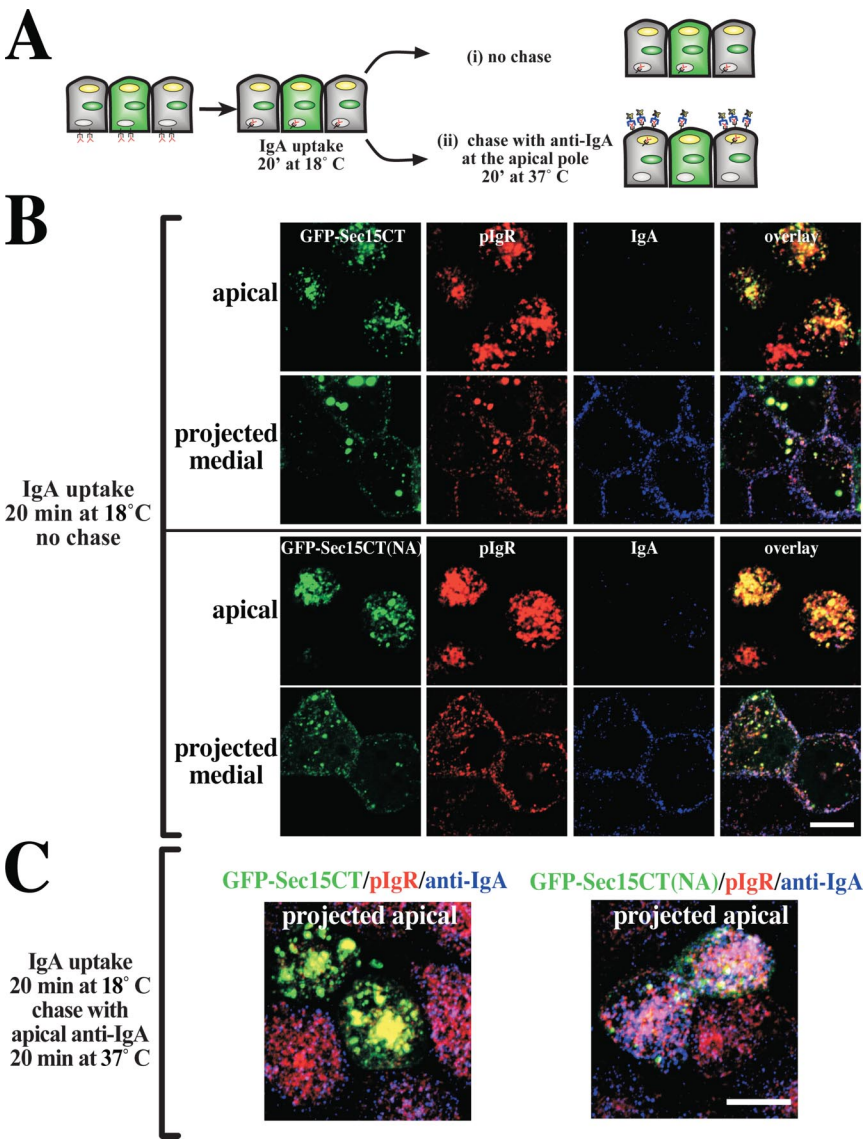

Figure 8. IgA transcytosis in polarized MDCK cells expressing GFP-Sec15CT or GFP-Sec15CT(NA). (A) Protocol for detecting basolaterally internalized IgA at the apical cell surface. (B) Distribution of GFP-Sec15CT or GFP-Sec15CT(NA) (green), the pIgR (red), and IgA (blue) endocytosed from the basolateral pole of the cell for 20 min at 18°C. An optical section from the apical pole of the cell and a projection of sections along the lateral region of the cell are shown. (C) IgA was internalized from the basolateral pole of the cell for 20 min at 18°C, and the cells were washed and then chased in for 20 min at 37°C. CY3-labeled anti-IgA antibodies were included in the apical medium during the incubation at 37°C. The distribution of GFP-Sec15CT or GFP-Sec15CT(NA) (green), pIgR (red), and anti-IgA (blue) is shown in projected optical sections taken from the apical pole of the cell.

compartment in a Rab11a-independent manner. However the mutant did not induce the formation of large vesicular structures in the medial cytoplasm and appeared to be predominantly cytoplasmic.

Next, we examined whether expression of GFP-Sec15CT altered basolateral-to-apical transcytosis of IgA using a morphological assay that scored the delivery of basolaterally internalized IgA to the apical surface of polarized MDCK cells (Figure 8A). IgA was internalized from the basolateral surface of the cells for 20 min at 18°C to trap a cohort of IgA in BEE (Song *et al.*, 1994). After this pulse, we confirmed that basolaterally internalized IgA was found in BEE subjacent to the basolateral surface of the cells expressing either GFP-Sec15CT or GFP-Sec15CT(NA) (see medial projections, Figure 8B). The cells were also labeled with an anti-pIgR mAb (SC166) to confirm pIgR expression. To initiate transcytosis, the basolateral surfaces of the cell were washed, and the cells were incubated in the absence of ligand for 20 min at 37°C. A Cy3-labeled secondary antibody specific for IgA was included in the apical medium during the 37°C chase to label IgA-bound pIgR complexes as they appeared at the apical cell surface (Figure 8A). As described above, a significant fraction of the pIgR escapes cleavage and recycles at the apical pole of the cell. After the chase in the presence of anti-IgA antibody, the cells were washed, fixed, and stained. We observed that in cells expressing GFP-Sec15CT, there was little uptake of Cy3-labeled secondary antibody (Figure 8C, blue), whereas in untransfected cells or those transfected with GFP-Sec15CT(NA), significant uptake of the anti-IgA antibody was detected at the apical pole of the cells (Figure 8C, blue), which colocalized with the pIgR. These results indicate that the expression of GFP-Sec15CT inhibited IgA delivery to the apical surface of the cell, whereas Sec15CT(NA), which binds inefficiently to Rab11a, had less of an effect. We also examined the effect of expressing GFP fused to full-length Sec15A; however, our analysis was thwarted by preliminary studies that showed expression of this construct resulted in the rapid formation of apoptotic cells, which had very low pIgR expression.

As further evidence of the effects of Sec15CT on transcytotic traffic, we used the stable MDCK cells lines expressing GFP-Sec15CT or GFP-Sec15CT(NA) described above. The level of expression of these two constructs was approximately equivalent to that of the endogenous protein (Figure

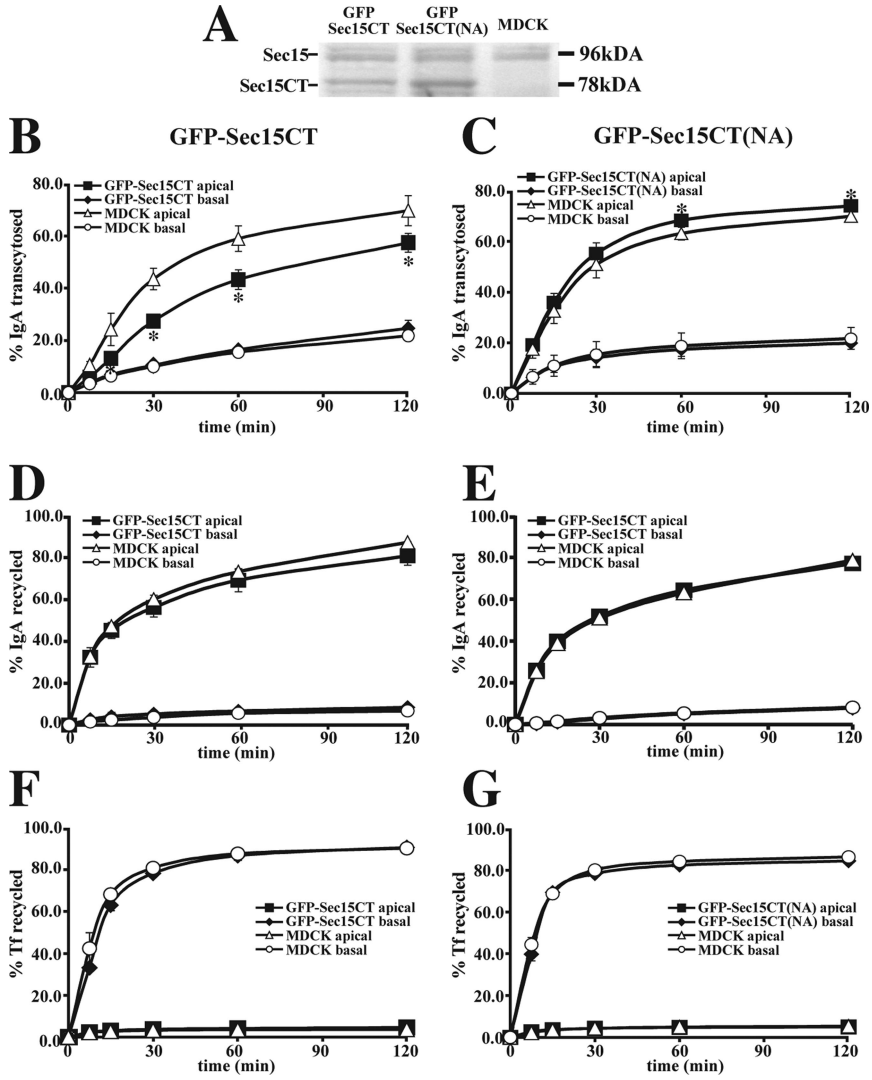

Figure 9. Effect of expressing GFP-Sec15CT and GFP-Sec15CT(NA) on the postendocytic fate of IgA and Tf in polarized MDCK cells infected with adenovirus encoding the pIgR. (A) Lysates of cells expressing GFP-Sec15CT or GFP-Sec15CT(NA) were resolved by SDS-PAGE, and Western blots were probed with an antibody against Sec15A. (B and C) Fate of basolaterally internalized ^{125}I-IgA in control MDCK cells or those expressing GFP-Sec15CT or GFP-Sec15CT(NA) (B and C, respectively). (D–E) Fate of apically internalized ^{125}I-IgA in control MDCK cells or those expressing GFP-Sec15CT or GFP-Sec15CT(NA) (D and E, respectively). (F and G) Fate of basolaterally internalized ^{125}I-Tf in control MDCK cells or those expressing GFP-Sec15CT or GFP-Sec15CT(NA) (F and G, respectively). In each panel, the fraction of ligand released from the apical or basal pole of the cell is shown. Data are mean ± SEM ($n \geq 2$; performed in triplicate). *Values are significantly different ($p < 0.05$) from those observed in control MDCK cells.

9A), which is likely to be an underestimate as only ~ 40–50% of the cells expressed these constructs, and was less than that observed using the transient transfection protocol described above. The medial vesicular structures were present in these cells, but were somewhat smaller in dimension, likely reflecting the lower levels of GFP-Sec15CT expression in these cell lines. To measure transcytosis, the cells were first infected with an adenovirus encoding the pIgR. After 24 h to allow for receptor expression, ^{125}I-IgA was internalized from the basolateral surface of the cell for 10 min at 37°C, the cells were washed, and the percentage of internalized ^{125}I-IgA released into the basolateral medium (recycled) or apical medium (transcytosed) was measured during a 2-h incubation at 37°C. Consistent with the morphological assay, we observed that IgA transcytosis was significantly impaired by expression of GFP-Sec15CT. The effect was kinetic with an ~50% inhibition observed at 15 min and ~20% at the 2-h time point (Figure 9B). There was little effect on basolateral recycling or degradation, but there was a compensatory increase in the amount of cell-associated ligand after the 2-h chase (data not shown). In contrast, there was no effect on apical recycling of IgA (Figure 9D) or basolateral recycling of Tf (Figure 9F). Expression of GFP-Sec15CT(NA) resulted in a small but significant stimulation of basolateral-to-apical transcytosis of IgA (Figure 9C), but had no effect on apical recycling of ^{125}I-IgA (Figure 9E), or basolateral recycling of ^{125}I-Tf (Figure 9G).

As a final experiment we down-regulated expression of Sec15A by transiently expressing a plasmid (pSuper-Sec15A) that expresses a Sec15A specific shRNA. Compared with cells expressing vector alone (not shown) or a control construct (pSuper-control), expression of pSuper-Sec15A resulted in a decrease in both Sec15A mRNA and protein expression as assessed by RT-PCR analysis or by Western blotting (Figure 10A). The decrease in protein and mRNA expression was somewhat variable (see triplicate samples in Figure 10A). By comparing the average amount of mRNA/protein found in cells expressing pSuper-Sec15A to cells expressing pSuper-control, we estimate that expression of pSuper-Sec15A decreased Sec15A mRNA expression by ~80% and Sec15A protein expression by ~50%. We used RT-PCR to confirm that pSuper-Sec15A had little effect on mRNA expression for Sec15B (Figure 10A; decrease of ~20%); however, the lack of isoform specific antibodies prevented us from examining the protein levels of Sec15B in the cells. There was no effect of silencing Sec15A expression on levels of Sec8 (Figure 10A). Expression of pSuper-Sec15A shRNA, but not pSuper-control, had a similar phenotype to

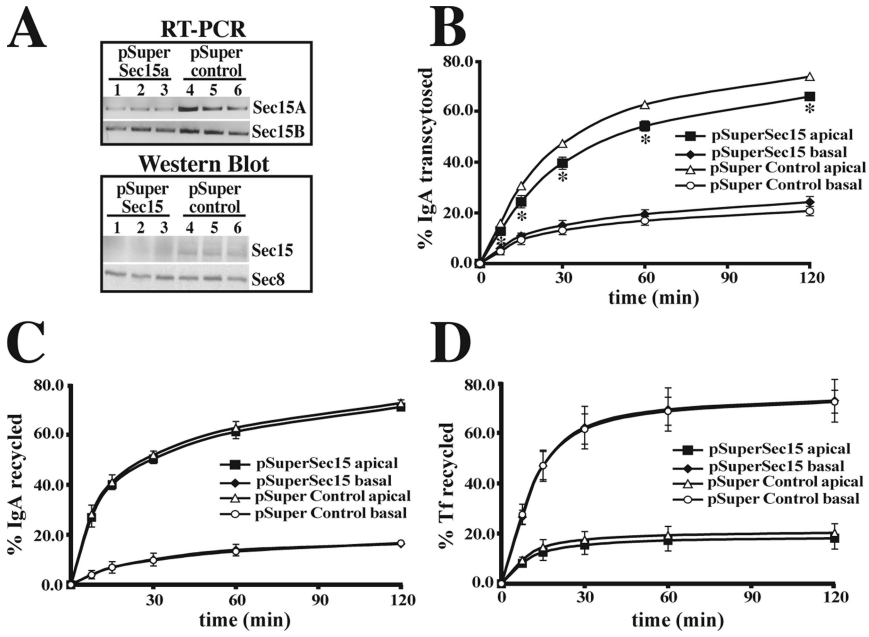

Figure 10. Dependence of basolateral-to-apical transcytosis on expression of Sec15A. (A) The upper panel shows Sec15A or Sec15B mRNA expression in three cell samples expressing pSuper-Sec15A (lanes 1–3) or pSuper-control (lanes 4–6). The lower panel shows a Western blot of lysates prepared from three cell samples expressing pSuper-Sec15A (lanes 1–3) or pSuper-control (lanes 4–6). The Western blot was sequentially probed with antibodies to Sec15A and then Sec8. (B) Basolateral-to-apical transcytosis of ^{125}I-IgA in cells expressing pSuper-Sec15A or pSuper-control. Shown is the amount of ligand released in the apical or basal chamber of the Transwell. (C) Apical recycling of ^{125}I-IgA in cells expressing pSuper-Sec15A or pSuper-control. (D) Basolateral recycling of ^{125}I-Tf in cells expressing pSuper-Sec15A or pSuper-control. Data are mean ± SEM ($n \geq 3$; performed in triplicate). *Values are significantly different ($p < 0.05$) from those observed in cells expressing pSuper-control.

expression of GFP-Sec15CT: basolateral-to-apical transcytosis was significantly inhibited at all time points (Figure 10B), but there was no effect on apical or basolateral recycling (Figure 10, C and D). Taken together, the above results indicate that Sec15A, possibly acting through Rab11a, modulates basolateral-to-apical transcytosis in polarized MDCK cells.

DISCUSSION

In mammalian epithelial cells, the octameric exocyst complex was generally thought to specifically direct fusion of cargo carriers with the basolateral pole of the cell (Grindstaff *et al.*, 1998; Munson and Novick, 2006). In contrast, we observed that 1) the exocyst is associated with both apical and basolateral endocytic compartments, 2) the exocyst regulates endocytic traffic directed toward both the basolateral and apical pole of the cell, and 3) the exocyst, Sec15A in particular, may function in association with Rab11a to regulate basolateral-to-apical transcytosis. Our results indicate that the exocyst is a general factor necessary for polarized endocytic traffic directed toward either pole of the epithelial cell and that pathway-selective traffic is likely to depend on association of the exocyst with distinct Ras family GTPases.

Localization of Exocyst to Multiple Endocytic Compartments in Polarized MDCK Cells

We examined the distribution of Sec6, Sec8, and Exo70 in polarized MDCK cells using antibodies and fixation conditions that revealed a tubulovesicular pool of these proteins. In contrast to previous reports showing exocyst subunit localization to the Golgi or TGN of NRK and subconfluent MDCK cells (Yeaman *et al.*, 2001; Prigent *et al.*, 2003), we generally did not observe colocalization between exocyst subunits and the TGN marker furin. This may reflect cell type differences or the use of different antibodies and fixation conditions. Consistent with previous studies (Folsch *et al.*, 2003; Prigent *et al.*, 2003), we observed that Sec6, Sec8, and Exo70 all colocalized with basolaterally internalized Tf in what appeared to be BEE and the CRE. Although Sec6 and Sec8 showed little association with EEA1, Exo70 appeared to distribute to the periphery of these early endosomal structures. Work in *Drosophila* has previously established that the distribution of individual exocyst components is not always identical (Beronja *et al.*, 2005; Murthy *et al.*, 2005). The function of Exo70 in early endosomes is unknown but the absence of Sec6 or Sec8 may indicate that Exo70 is acting independently or as part of a subcomplex. An alternative possibility is that Exo70 is marking the site of assembly of the octameric exocyst complex, a function proposed for Exo70p in yeast (Boyd *et al.*, 2004).

The recent finding that Rab11 interacts with Sec15 (Zhang *et al.*, 2004; Wu *et al.*, 2005) prompted us to also explore whether exocyst subunits associated with the Rab11a-positive ARE, an endosome that regulates apically directed endocytic traffic in MDCK cells (Casanova *et al.*, 1999; Wang *et al.*, 2000b). Indeed, we observed a fraction of exocyst subunits that colocalized with Rab11a in the apical region of polarized MDCK cells. There was a pool of exocyst subunits that did not colocalize with any of the markers we used and may represent exocyst association with other organelles such as the endoplasmic reticulum (Lipschutz *et al.*, 2003). Taken together, the data indicate that the exocyst localizes to multiple endocytic compartments, including those involved in traffic directed toward both the basolateral and apical poles of the polarized MDCK cell.

Requirement for Exocyst in Both Basolateral- and Apical-directed Endocytic Transport

Although not all membrane trafficking steps are dependent on the exocyst (Grindstaff *et al.*, 1998; Murthy *et al.*, 2003; Clandinin, 2005), the association of the exocyst with multiple endocytic compartments indicated that it may be involved in a broader range of trafficking events than originally proposed. To examine this possibility, we reconstituted endocytic trafficking events in SLO-permeabilized cells. Consistent with the localization of exocyst subunits to Tf-positive endosomes, we observed that a cocktail of function-blocking Sec8 antibodies significantly inhibited basolateral recycling of Tf. The inhibition of Tf recycling was not complete, per-

haps indicating that the blocking antibodies had access to only a subset of exocyst complexes involved in recycling or that Tf recycling is occurring by more than one mechanism. Although previous studies showed that Tf recycling is exocyst dependent in nonpolarized cells and that the exocyst is localized to recycling endosomes in MDCK cells (Folsch *et al.*, 2003; Prigent *et al.*, 2003), it was unknown whether basolateral recycling was exocyst dependent in polarized epithelial cells.

By staging IgA in the ARE before reconstitution, we further showed that a late step in the basolateral-to-apical transcytotic pathway, namely movement from ARE to the apical plasma membrane, was sensitive to function-blocking Sec8 antibodies. Again, the inhibition was not complete, and this may again reflect issues of antibody access or of a multiplicity of mechanisms and/or pathways. Because the ARE is located just below the apical plasma membrane, the inhibition we observed is consistent with current models in which the exocyst promotes tethering at the plasma membrane. However, our finding that vesicle budding also showed some dependence on the exocyst indicates that the exocyst may also play some role in steps that precede vesicle fusion, possibly including cargo selection or vesicle transport. It was previously reported that function-blocking antibodies against Sec6/Sec8 inhibit cargo exit from the TGN (Grindstaff *et al.*, 1998; Yeaman *et al.*, 2001), and expression of mutant alleles of Sec5, Sec6, or Sec15 result in accumulation of DE-cadherin in Rab11-positive endosomes (Langevin *et al.*, 2005), and not, for example, in vesicles near the plasma membrane. It is interesting to note that the octameric conserved oligomeric Golgi (COG) complex, which regulates a variety of functions (cargo sorting, vesicle trafficking/tethering) in different intracellular compartments (ER, Golgi, and endosomes), shares structural and sequence similarities to the exocyst (Oka and Krieger, 2005). Thus, the exocyst may also regulate multiple membrane traffic steps in the endocytic/biosynthetic systems, including ones we did not examine in this study.

We also examined whether the exocyst was involved in apical recycling of IgA. Unlike basolateral-to-apical transcytosis of IgA (and Tf recycling), we observed that inhibition of apical recycling by function-blocking Sec8 antibodies was almost complete, indicating that the mechanism of apical IgA recycling is highly dependent on Sec8 function. This disparity may reflect differences in the pathways/mechanisms that the two populations of receptors employ or interactions between the pIgR and distinct classes of sorting machineries, some of which may not be dependent on Sec8 or are not affected by the addition of anti-Sec8 antibodies (see also discussion below). Our observation that the exocyst is important for apically directed traffic is consistent with observations that the exocyst is important for delivery of cargo to the apical membrane-associated rhabdomeres of epithelial photoreceptor cells in *Drosophila* (Beronja *et al.*, 2005).

Sec15A-Rab11a Requirement for Basolateral-to-Apical Transcytosis

The association of the exocyst with multiple intracellular compartments and the dependence of multiple trafficking steps on exocyst function indicate that there must be a mechanism(s) to affect exocyst localization and exploit its functions in a pathway-specific manner. Likely players in this regard include a growing list of Ras family GTPases that interact with various exocyst subunits in metazoans: Arf6 with Sec10; RalA/RalB with Sec5 and Exo84; Tc10 with Exo70; and Rab11 with Sec15 (Grosshans *et al.*, 2006; Munson and Novick, 2006). Small GTPases exhibit a highly specialized distribution in the cell and are involved in recruiting effector proteins to intracellular compartments.

Confirming previous reports (Zhang *et al.*, 2004; Wu *et al.*, 2005), we observed that Rab11a interacts with the C-terminus of Sec15A. Our analysis further demonstrated that the GFP-tagged Sec15A C-terminus was associated with Rab11a-positive endosomes, that it caused the accumulation of Rab11a in large vesicular structures, and that it acted as a dominant-negative inhibitor of basolateral-to-apical transcytosis. In contrast, this mutant had no effect on the basolateral recycling pathway, which was previously shown to be independent of Rab11a (Wang *et al.*, 2000b). Inhibition of transcytosis was not observed when we expressed the GFP-Sec15CT(NA) mutant, which blocks interactions between the Sec15A C-terminus and Rab11a. The *Drosophila* Sec15 C-terminus also binds to Rab3, Rab8, and Rab27 in two-hybrid assays (Wu *et al.*, 2005). As such, we cannot exclude the possibility that GFP-Sec15CT expression may cause inhibition as a result of its interactions with other GTPases. However, there is no evidence as yet that the exocyst interacts with these GTPases in vivo, nor is it known whether they bind to Sec15CT at the same site as Rab11a. Furthermore, although there is some evidence that Rab3b regulates transcytosis (van IJzendoorn *et al.*, 2002), Rab8 is generally thought to regulate basolateral events (Ang *et al.*, 2003), and there is no evidence that Rab27a/b are expressed in MDCK cells. Although our data are consistent with a model whereby Rab11a recruits the exocyst via Sec15A to modulate transcytotic traffic, we cannot exclude a role for the closely related Rab11b isoform that shares many of the same effectors as Rab11a. However, Rab11b localization is distinct from that of Rab11a and Rab11b does not colocalize with Tf or the pIgR in polarized MDCK cells (Lapierre *et al.*, 2003).

Consistent with the observations described above, we found that down-regulation of Sec15A, using shRNA, inhibited basolateral-to-apical transcytosis, but did not affect receptor recycling pathways. The inhibition of transcytosis most likely reflected defects in the movement into or out of the Rab11a-positive elements of the ARE. However, it is possible that earlier trafficking steps were also affected. The inhibition of transcytosis was modest, possibly reflecting our inability to achieve complete Sec15A knockdown or the possibility that there may be alternative mechanisms/pathways for transcytosis. An additional possibility is that Sec15B may compensate for the loss of Sec15A (however, see *Discussion* below for an alternative possibility). Unfortunately, there are few reagents to study Sec15B at present, so the role of this isoform in endocytic traffic is left to future studies.

The lack of effect of expressing GFP-Sec15CT or pSuper-Sec15A on apical IgA recycling was surprising as both apical recycling and basolateral-to-apical transcytosis are regulated by Rab11a (Wu *et al.*, 2005), and we confirmed that expression of GFP/HA-Rab11aSN inhibited both of these pathways (Oztan and Apodaca, unpublished observations). A likely possibility is that Rab11a regulates these two pathways through recruitment of a distinct subset of effectors or their functions. Consistent with this possibility we recently observed that the SARG and Δ C mutants of Rab11-interacting protein 2 affect basolateral-to-apical transcytosis, but have no impact on apical recycling (Ducharme *et al.*, 2007), and other studies have noted differences between apical IgA recycling and basolateral-to-apical transcytosis of this ligand (Low *et al.*, 1998; Wu *et al.*, 2005). The data presented in this article indicates that the Rab11a-Sec15A interaction may be specific for the basolateral-to-apical transcytotic pathway.

However, because we did not achieve complete knockdown of Sec15A expression, we cannot rule out that further down-regulation of Sec15A may impact other trafficking pathways including receptor recycling.

There are additional explanations for why Sec15A may selectively regulate basolateral-to-apical transcytosis and not other exocyst-dependent endocytic trafficking pathways. One possibility is that there are distinct exocyst holocomplexes containing either Sec15A or Sec15B subunits and the complex containing Sec15A is selectively involved in regulating the basolateral-to-apical transcytotic pathway. An alternative possibility is that there are "physically distinct subcomplexes" comprised of a subset of exocyst subunits, which would function independent of the holocomplex and would act downstream of GTPases such as Rab11a to regulate basolateral-to-apical transcytosis. In yeast, Sec15p and Sec10p form a subcomplex found in the cytosol as well as part of the holocomplex (Guo *et al.*, 1999), and in mammalian cells Sec10 and Exo84 (and presumably Sec15) may form a similar subcomplex (Moskalenko *et al.*, 2003). However, it is unknown whether the Sec10/Sec15/Exo84 subcomplex is functionally active, or if it modulates distinct trafficking events. Our finding that multiple exocyst subunits are found on the ARE and CRE suggest an additional possibility: the exocyst may form "functionally distinct subcomplexes." In this case all subunits are present in the octameric complex; however, the functionally active ones depend on their cellular localization and association with regulatory GTPases. Thus Rab11a could recruit the exocyst holocomplex via Sec15A and then modulate Sec15A function to promote basolateral-to-apical transcytosis. Although these models are not mutually exclusive, they suggest ways that the exocyst subunits, either as part of the holocomplex or part of physically distinct subcomplexes, may act downstream of compartment-specific GTPases such as Rab11a to modulate specific cellular events such as basolateral-to-apical transcytosis.

ACKNOWLEDGMENTS

We kindly thank Elena Balestreire, Dr. Christine Rondanino, and Dr. Linton Traub for helpful discussions and critical review of the manuscript. We thank Dr. Robert Edinger for the GFP/HA-Rab11a adenovirus, Jennifer R. Bruns (University of Pittsburgh) for the pIgR and AvTA adenoviruses, and Chris Guerriero for his assistance in live cell imaging and shRNA studies. This work was supported by a Predoctoral Fellowship from the American Heart Association to A.O. (0615440U), an Established Investigator Award to G.A from the American Heart Association (0340021), and National Institutes of Health grants to O.A.W (DK-54407), S.C.H. (NS0-38892), J.R.G. (DK-070856, DK-48370, and DK-43405), C.Y. (NIGMS-67002), and G.A. (DK-51970 and DK-54425).

REFERENCES

Altschuler, Y., Kinlough, C. L., Poland, P. A., Bruns, J. B., Apodaca, G., Weisz, O. A., and Hughey, R. P. (2000). Clathrin-mediated endocytosis of MUC1 is modulated by its glycosylation state. Mol. Biol. Cell *11*, 819–831.

Ang, A. L., Folsch, H., Koivisto, U. M., Pypaert, M., and Mellman, I. (2003). The Rab8 GTPase selectively regulates AP-1B-dependent basolateral transport in polarized Madin-Darby canine kidney cells. J. Cell Biol. *163*, 339–350.

Ang, A. L., Taguchi, T., Francis, S., Folsch, H., Murrells, L. J., Pypaert, M., Warren, G., and Mellman, I. (2004). Recycling endosomes can serve as intermediates during transport from the Golgi to the plasma membrane of MDCK cells. J. Cell Biol. *167*, 531–543.

Apodaca, G., Cardone, M. H., Whiteheart, S. W., DasGupta, B. R., and Mostov, K. E. (1996). Reconstitution of transcytosis in SLO-permeabilized MDCK cells: existence of an NSF-dependent fusion mechanism with the apical surface of MDCK cells. EMBO J. *15*, 1471–1481.

Apodaca, G., Katz, L. A., and Mostov, K. E. (1994). Receptor-mediated transcytosis of IgA in MDCK cells is via apical recycling endosomes. J. Cell Biol. *125*, 67–86.

Bacallao, R., and Stelzer, E. H. (1989). Preservation of biological specimens for observation in a confocal fluorescence microscope and operational principles of confocal fluorescence microscopy. Methods Cell Biol. *31*, 437–452.

Barile, M., Pisitkun, T., Yu, M. J., Chou, C. L., Verbalis, M. J., Shen, R. F., and Knepper, M. A. (2005). Large scale protein identification in intracellular aquaporin-2 vesicles from renal inner medullary collecting duct. Mol. Cell Proteomics *4*, 1095–1106.

Beronja, S., Laprise, P., Papoulas, O., Pellikka, M., Sisson, J., and Tepass, U. (2005). Essential function of *Drosophila* Sec6 in apical exocytosis of epithelial photoreceptor cells. J. Cell Biol. *169*, 635–646.

Bomsel, M., and Mostov, K. E. (1993). Possible role of both the alpha and beta gamma subunits of the heterotrimeric G protein, Gs, in transcytosis of the polymeric immunoglobulin receptor. J. Biol. Chem. *268*, 25824–25835.

Boyd, C., Hughes, T., Pypaert, M., and Novick, P. (2004). Vesicles carry most exocyst subunits to exocytic sites marked by the remaining two subunits, Sec3p and Exo70p. J. Cell Biol. *167*, 889–901.

Breitfeld, P. P., Harris, J. M., and Mostov, K. E. (1989). Postendocytotic sorting of the ligand for the polymeric immunoglobulin receptor in Madin-Darby canine kidney cells. J. Cell Biol. *109*, 475–486.

Brown, P. S., Wang, E., Aroeti, B., Chapin, S. J., Mostov, K. E., and Dunn, K. W. (2000). Definition of distinct compartments in polarized Madin-Darby canine kidney (MDCK) cells for membrane-volume sorting, polarized sorting and apical recycling. Traffic *1*, 124–140.

Casanova, J. E., Wang, X., Kumar, R., Bhartur, S. G., Navarre, J., Woodrum, J. E., Altschuler, Y., Ray, G. S., and Goldenring, J. R. (1999). Association of Rab25 and Rab11a with the apical recycling system of polarized Madin-Darby canine kidney cells. Mol. Biol. Cell *10*, 47–61.

Clandinin, T. R. (2005). Surprising twists to exocyst function. Neuron *46*, 164–166.

Ducharme, N., Williams, J., Oztan, A., Apodaca, G., and Goldenring, J. (2007). RAB11-FIP2 regulates differentiable steps in transcytosis. Am. J. Physiol. Cell Physiol. (*in press*).

Folsch, H., Pypaert, M., Maday, S., Pelletier, L., and Mellman, I. (2003). The AP-1A and AP-1B clathrin adaptor complexes define biochemically and functionally distinct membrane domains. J. Cell Biol. *163*, 351–362.

Gorvel, J. P., Chavrier, P., Zerial, M., and Gruenberg, J. (1991). rab5 controls early endosome fusion in vitro. Cell *64*, 915–925.

Grindstaff, K. K., Yeaman, C., Anandasabapathy, N., Hsu, S. C., Rodriguez-Boulan, E., Scheller, R. H., and Nelson, W. J. (1998). Sec6/8 complex is recruited to cell-cell contacts and specifies transport vesicle delivery to the basal-lateral membrane in epithelial cells. Cell *93*, 731–740.

Grosshans, B. L., Ortiz, D., and Novick, P. (2006). Rabs and their effectors: achieving specificity in membrane traffic. Proc. Natl. Acad. Sci. USA *103*, 11821–11827.

Guo, W., Roth, D., Walch-Solimena, C., and Novick, P. (1999). The exocyst is an effector for Sec4p, targeting secretory vesicles to sites of exocytosis. EMBO J. *18*, 1071–1080.

Henkel, J. R., Apodaca, G., Altschuler, Y., Hardy, S., and Weisz, O. A. (1998). Selective perturbation of apical membrane traffic by expression of influenza M2, an acid-activated ion channel, in polarized madin-darby canine kidney cells. Mol. Biol. Cell *9*, 2477–2490.

Jafar-Nejad, H., Andrews, H. K., Acar, M., Bayat, V., Wirtz-Peitz, F., Mehta, S. Q., Knoblich, J. A., and Bellen, H. J. (2005). Sec15, a component of the exocyst, promotes notch signaling during the asymmetric division of *Drosophila* sensory organ precursors. Dev. Cell *9*, 351–363.

Langevin, J., Morgan, M. J., Sibarita, J. B., Aresta, S., Murthy, M., Schwarz, T., Camonis, J., and Bellaiche, Y. (2005). *Drosophila* exocyst components Sec5, Sec6, and Sec15 regulate DE-Cadherin trafficking from recycling endosomes to the plasma membrane. Dev. Cell *9*, 355–376.

Lapierre, L. A., Dorn, M. C., Zimmerman, C. F., Navarre, J., Burnette, J. O., and Goldenring, J. R. (2003). Rab11b resides in a vesicular compartment distinct from Rab11a in parietal cells and other epithelial cells. Exp. Cell Res. *290*, 322–331.

Leung, S. M., Chen, D., DasGupta, B. R., Whiteheart, S. W., and Apodaca, G. (1998). SNAP-23 requirement for transferrin recycling in Streptolysin-O-permeabilized Madin-Darby canine kidney cells. J. Biol. Chem. *273*, 17732–17741.

Leung, S. M., Ruiz, W. G., and Apodaca, G. (2000). Sorting of membrane and fluid at the apical pole of polarized Madin-Darby canine kidney cells. Mol. Biol. Cell *11*, 2131–2150.

Lipschutz, J. H., Guo, W., O'Brien, L. E., Nguyen, Y. H., Novick, P., and Mostov, K. E. (2000). Exocyst is involved in cystogenesis and tubulogenesis and acts by modulating synthesis and delivery of basolateral plasma membrane and secretory proteins. Mol. Biol. Cell *11*, 4259–4275.

Lipschutz, J. H., Lingappa, V. R., and Mostov, K. E. (2003). The exocyst affects protein synthesis by acting on the translocation machinery of the endoplasmic reticulum. J. Biol. Chem. *278*, 20954–20960.

Low, S. H., Chapin, S. J., Wimmer, C., Whiteheart, S. W., Komuves, L. G., Mostov, K. E., and Weimbs, T. (1998). The SNARE machinery is involved in apical plasma membrane trafficking in MDCK cells. J. Cell Biol. *141*, 1503–1513.

Maples, C. J., Ruiz, W. G., and Apodaca, G. (1997). Both microtubules and actin filaments are required for efficient postendocytotic traffic of the polymeric immunoglobulin receptor in polarized Madin-Darby canine kidney cells. J. Biol. Chem. *272*, 6741–6751.

Moskalenko, S., Tong, C., Rosse, C., Mirey, G., Formstecher, E., Daviet, L., Camonis, J., and White, M. A. (2003). Ral GTPases regulate exocyst assembly through dual subunit interactions. J. Biol. Chem. *278*, 51743–51748.

Munson, M., and Novick, P. (2006). The exocyst defrocked, a framework of rods revealed. Nat. Struct. Mol. Biol. *13*, 577–581.

Murthy, M., Garza, D., Scheller, R. H., and Schwarz, T. L. (2003). Mutations in the exocyst component Sec5 disrupt neuronal membrane traffic, but neurotransmitter release persists. Neuron *37*, 433–447.

Murthy, M., Ranjan, R., Denef, N., Higashi, M. E., Schupbach, T., and Schwarz, T. L. (2005). Sec6 mutations and the *Drosophila* exocyst complex. J. Cell Sci. *118*, 1139–1150.

Oka, T., and Krieger, M. (2005). Multi-component protein complexes and Golgi membrane trafficking. J. Biochem. (Tokyo) *137*, 109–114.

Prigent, M., Dubois, T., Raposo, G., Derrien, V., Tenza, D., Rosse, C., Camonis, J., and Chavrier, P. (2003). ARF6 controls post-endocytic recycling through its downstream exocyst complex effector. J. Cell Biol. *163*, 1111–1121.

Ren, M., Xu, G., Zeng, J., De Lemos-Chiarandini, C., Adesnik, M., and Sabatini, D. D. (1998). Hydrolysis of GTP on rab11 is required for the direct delivery of transferrin from the pericentriolar recycling compartment to the cell surface but not from sorting endosomes. Proc. Natl. Acad. Sci. USA *95*, 6187–6192.

Rogers, K. K., Jou, T. S., Guo, W., and Lipschutz, J. H. (2003). The Rho family of small GTPases is involved in epithelial cystogenesis and tubulogenesis. Kidney Int. *63*, 1632–1644.

Rogers, K. K., Wilson, P. D., Snyder, R. W., Zhang, X., Guo, W., Burrow, C. R., and Lipschutz, J. H. (2004). The exocyst localizes to the primary cilium in MDCK cells. Biochem. Biophys. Res. Commun. *319*, 138–143.

Sheff, D. R., Daro, E. A., Hull, M., and Mellman, I. (1999). The receptor recycling pathway contains two distinct populations of early endosomes with different sorting functions. J. Cell Biol. *145*, 123–139.

Shin, D. M., Zhao, X. S., Zeng, W., Mozhayeva, M., and Muallem, S. (2000). The mammalian Sec6/8 complex interacts with Ca(2+) signaling complexes and regulates their activity. J. Cell Biol. *150*, 1101–1112.

Shipitsin, M., and Feig, L. A. (2004). RalA but not RalB enhances polarized delivery of membrane proteins to the basolateral surface of epithelial cells. Mol. Cell Biol. *24*, 5746–5756.

Song, W., Apodaca, G., and Mostov, K. (1994). Transcytosis of the polymeric immunoglobulin receptor is regulated in multiple intracellular compartments. J. Biol. Chem. *269*, 29474–29480.

Ullrich, O., Reinsch, S., Urbe, S., Zerial, M., and Parton, R. G. (1996). Rab11 regulates recycling through the pericentriolar recycling endosome. J. Cell Biol. *135*, 913–924.

van IJzendoorn, S. C., Tuvim, M. J., Weimbs, T., Dickey, B. F., and Mostov, K. E. (2002). Direct interaction between Rab3b and the polymeric immunoglobulin receptor controls ligand-stimulated transcytosis in epithelial cells. Dev. Cell *2*, 219–228.

Vega, I. E., and Hsu, S. C. (2001). The exocyst complex associates with microtubules to mediate vesicle targeting and neurite outgrowth. J. Neurosci. *21*, 3839–3848.

Wang, E., Brown, P. S., Aroeti, B., Chapin, S. J., Mostov, K. E., and Dunn, K. W. (2000a). Apical and basolateral endocytic pathways of MDCK cells meet in acidic common endosomes distinct from a nearly-neutral apical recycling endosome. Traffic *1*, 480–493.

Wang, S., and Hsu, S. C. (2006). The molecular mechanisms of the mammalian exocyst complex in exocytosis. Biochem. Soc. Trans. *34*, 687–690.

Wang, X., Kumar, R., Navarre, J., Casanova, J. E., and Goldenring, J. R. (2000b). Regulation of vesicle trafficking in madin-darby canine kidney cells by Rab11a and Rab25. J. Biol. Chem. *275*, 29138–29146.

Wilcke, M., Johannes, L., Galli, T., Mayau, V., Goud, B., and Salamero, J. (2000). Rab11 regulates the compartmentalization of early endosomes required for efficient transport from early endosomes to the trans-golgi network. J. Cell Biol. *151*, 1207–1220.

Wu, S., Mehta, S. Q., Pichaud, F., Bellen, H. J., and Quiocho, F. A. (2005). Sec15 interacts with Rab11 via a novel domain and affects Rab11 localization in vivo. Nat. Struct. Mol. Biol. *12*, 879–885.

Yeaman, C., Grindstaff, K. K., and Nelson, W. J. (1999). New perspectives on mechanisms involved in generating epithelial cell polarity. Physiol. Rev. *79*, 73–98.

Yeaman, C., Grindstaff, K. K., and Nelson, W. J. (2004). Mechanism of recruiting Sec6/8 (exocyst) complex to the apical junctional complex during polarization of epithelial cells. J. Cell Sci. *117*, 559–570.

Yeaman, C., Grindstaff, K. K., Wright, J. R., and Nelson, W. J. (2001). Sec6/8 complexes on trans-Golgi network and plasma membrane regulate late stages of exocytosis in mammalian cells. J. Cell Biol. *155*, 593–604.

Zhang, X. M., Ellis, S., Sriratana, A., Mitchell, C. A., and Rowe, T. (2004). Sec15 is an effector for the Rab11 GTPase in mammalian cells. J. Biol. Chem. *279*, 43027–43034.